ORIGINAL PAPER

Beneficial effects of curcumin in the diabetic rat ovary: a stereological and biochemical study

Kıymet Kubra Tufekci[1] · Suleyman Kaplan[2]

Abstract

This study aimed to investigate the effects of curcumin treatment on ovaries at different periods of the diabetes disease. Fifty-six female Wistar albino rats (250–300 g) aged 12 weeks were divided into seven groups. No treatment was applied to the control group. The sham group was given 5 mL/kg of corn oil, and the curcumin group 30 mg/kg curcumin. In the diabetes mellitus (DM) groups, diabetes was induced by a single intraperitoneal dose of 50 mg/kg streptozotocin (STZ). The DM-treated groups received 30 mg/kg curcumin after either 7 days (DC1 group) or 21 days (DC2 group), or simultaneously with STZ injection (DC3 group). Number of follicles in the ovaries was estimated using stereological method. Follicle-stimulating hormone (FSH), luteinizing hormone (LH), and superoxide dismutase (SOD) levels and catalase (CAT) activity were measured in serum specimens. We found that follicle number and volume of corpus luteum, blood vessel, and cortex, gonadosomatic index, and FSH and SOD levels all decreased significantly in diabetic ovaries, while relative weight loss, connective tissue volume, and CAT activity increased ($p < 0.01$). Curcumin treatment had a protective effect on the number of primordial follicles in the DC2 group and on antral follicle numbers in the DC3 group. Curcumin also exhibited positive effects on CAT activity and SOD levels, blood glucose levels, and corpus luteum, connective tissue, and blood vessel volumes in the DC2 and DC3 groups. Curcumin also ameliorated FSH levels in the DC1 and DC3 groups ($p < 0.01$). These findings suggest that curcumin exhibits protective effects on ovarian structures and folliculogenesis, especially when used concurrently with the development of diabetes or in later stages of the disease.

Keywords Antioxidant · Diabetes · Curcumin · Oxidative stress · Stereology · Follicle number

Introduction

Diabetes mellitus (DM) is a metabolic disease whose development involves both hereditary and environmental factors. It is characterized by excessive blood glucose levels and can result in various complications, such as retinopathy, nephropathy, neuropathy, and cardiovascular diseases (Herman 2007). DM has also been reported to adversely affect both male and female reproductive activities (Wu et al. 2017). Delayed oocyte maturation and stages of meiosis, increased follicular and granulosa cell apoptosis, disorders in oocyte–granulosa communication and follicle development,

estrus cycle disruptions (especially oligomenorrhea), anovulation, decreased mating ability, mild hyperandrogenism, polycystic ovary syndrome, a decreased live birth rate, and early menopause have been observed in diabetic rats (Codner et al. 2012). Insulin stimulates the secretory activity of the gonadotropic axis by directly affecting gonadotropin-releasing hormone (GnRH) neurons (increasing Kiss1/kisspeptin expressions) (Pralong 2010). Diabetes has been reported to suppress hypothalamic expression of the *Kiss1* gene in male and female rats treated with streptozotocin (STZ) (Castellano et al. 2009).

Although many mechanisms have been proposed to explain both the development of diabetes and the pathogenesis of its complications, the most important of these involves increased free radicals in tissue (Volpe et al. 2018). Studies have shown that individuals with diabetes are susceptible to oxidative stress. Increased free radicals in tissue as a result of high blood glucose levels are known to exacerbate lipid peroxidation. A decrease in

✉ Suleyman Kaplan
skaplanomu@yahoo.com; skaplan@omu.edu.tr

1 Department of Histology and Embryology, Faculty of Medicine, Kastamonu University, Kastamonu, Turkey

2 Department of Histology and Embryology, Faculty of Medicine, Ondokuz Mayıs University, Samsun, Turkey

intracellular antioxidant enzyme activities has also been reported as a result of diabetes (Kovacevic et al. 2022).

The principal aim of treatment is to minimize and delay complications caused by diabetes. Curcumin is a phenolic compound obtained from the roots of the turmeric plant and is known to exhibit positive effects on various chronic diseases associated with inflammation and oxidative stress (Soleimani et al. 2018). It has also been studied as a potential therapeutic agent in experimental diabetes and in the treatment of diabetic complications due to its effectiveness in reducing hyperglycemia and hyperlipidemia (Zhang et al. 2013).

Curcumin is recognized and used differently in many countries around the world. There are many studies on the health benefits of curcumin from the cellular level to animals, including human studies (Adab et al. 2019; Asadi et al. 2020; Xie et al. 2021). Studies have reported that curcumin has various biological and pharmacological properties including strong antioxidant, anti-inflammatory, immunomodulatory, antimicrobial, anti-ischemic, anticarcinogen, liver-protective, kidney-protective, antihyperglycemic, and antirheumatic activities (Liu et al. 2022). This compound also shows various therapeutic effects against various diseases, including anxiety, depression, metabolic syndrome, ulcer, osteoarthritis, and non-alcoholic fatty liver disease (Abu-Taweel and Rudayni 2022). According to studies investigating the safety of turmeric, commercially available curcumin contains about 77% curcumin, 17% de-methoxycurcumin, and 3% bisdemethoxycurcumin. The standardized powder and extract of curcumin are safe for human use, even at high doses of 6 g per day for 7 weeks (Marton et al. 2021). Thanks to its antioxidant properties, curcumin has an important role in preventing diabetes complications and significantly reducing the risk of development (Xie et al. 2021).

Curcumin suppresses lipid peroxidation and blood glucose levels in patients with diabetes, increases the function of pancreatic β-cells, and delays the production of reactive oxygen species (ROS) (Meghana et al. 2007; Perez-Torres et al. 2013; Marton et al. 2021). It is also thought to possess phytoestrogenic effects, and can therefore interact with the endocrine system, affecting the hypothalamic–pituitary–ovarian axis and repairing these disorders (Bachmeier et al. 2010). Curcumin shows therapeutic effects on polycystic ovary syndrome (PCOS), ovarian failure, and endometriosis (Kamal et al. 2021). In a rat model of ovarian ischemia–reperfusion injury, curcumin improved the oxidative status parameters (Behroozi-Lak et al. 2018). It has been reported that curcumin has efficacy in ovarian cancer carcinoma models through antitumorigenic and anti-angiogenic mechanisms. It is suggested that these effects are mediated by VEGF, NF-kB, IL-6, and matrix metalloproteinases (MMPs) (Lin et al. 2007).

Considering the effects of curcumin on fertility, it has been found to increase the number of offspring in rabbits, increasing oocyte production and growth by altering both the release of ovarian hormones and the response of the ovaries to gonadotropin. It has also been reported that curcumin protects mouse ovarian cells from the pro-apoptotic, pronecrotic, and antiproliferative effects of stress caused by the reduction of FSH receptors (Tiwari-Pandey and Ram Sairam 2009).

Although numerous studies have investigated the effects of DM on ovarian histopathology, the problem remains unsolved. Comprehensive studies are still needed in this area. The purpose of the present study was to determine the structural, functional, and hormonal changes occurring in the diabetic ovary and to investigate the possible protective effects and mechanisms of curcumin, with its potential antihyperglycemic and phytoestrogenic effects, on the diabetic ovary at the structural and biochemical levels.

An experimental animal model was employed to investigate how curcumin application to the diabetic ovaries would affect follicle count and volume, and blood vessel and connective tissue volumes in the ovary. These were investigated in a quantitative manner using the unbiased cell count method, the optical fractionator counting technique, and the Cavalieri principle. The stereological techniques used are design-based methods based on statistical principles (Boyce et al. 2010). In addition, the fact that these methods are based on the principle of impartiality further enhances the value and reliability of the data obtained (Gundersen 1986). The physiological effectiveness of curcumin administration on the hypothalamic–pituitary–gonadal axis in individuals with diabetes was also investigated in the present study. The fact that changing gonadotropin levels in individuals with diabetes can be regulated by curcumin treatment plays an important role in maintaining ovarian functions. Oxidative stress parameters were measured using biochemical techniques. This study also evaluated the biochemical effect of DM on reproductive activities and the protective antioxidant activity of curcumin.

The results of this study may encourage the use of curcumin to compensate for insulin resistance and hyperglycemia observed that are observed during the treatment of individuals with diabetes. We hope that our findings will contribute to the development of new therapeutic approaches in cases of diabetes-related infertility and to the reduction of ovarian toxicity or to the preservation of ovarian quality and reproductive activities in individuals with diabetes.

Materials and methods

Animals

All experimental procedures were carried out at the Ondokuz Mayıs University Experimental Animal

Application and Research Center (DEHAM), Turkey, following approval by the Ondokuz Mayıs University Experimental Animals Ethical Committee (no. 2017/53 dated 24 November 2017). The welfare of the experimental animals and relevant ethical principles were taken into account during the procedures performed throughout the experiment. The ARRIVE guidelines 2.0 (Animal Research: Reporting of In Vivo Experiments) were strictly followed while doing this experiment. The experimental animals were allowed ad libitum access to water and feed in a 12 h–12–h light–dark cycle at a room temperature of 22 ± 2 °C and relative humidity of 40–60%.

Experimental design

Fifty-six female Wistar albino female rats aged 12 weeks and weighing 250–300 g were used in the experiment. These were randomly divided into seven groups of eight animals each. In the experiment, we designed the diabetic + curcumin groups on the basis of these reasons: 7 days (DC1), to see protective effects of curcumin in the early stage of experimental diabetes, and 21 days (DC2), to simulate the long-term effects of experimental diabetes and curcumin relationship, while the DC3 group was designed to imitate protective effects of curcumin on the development and progression of experimental diabetes.

Group 1: control.

No procedure was performed on the animals in this group.

Group 2: sham.

Corn oil was administered by intragastric gavage for 14 days.

Group 3: curcumin.

Curcumin (Sigma-Aldrich, St Louis, MO, USA; C1386) (30 mg/kg) (Sharma et al. 2006) was dissolved in corn oil and administered by intragastric gavage for 14 days.

Group 4: diabetes mellitus group.

Diabetes was induced with a single intraperitoneal dose of 50 mg/kg STZ (Cayman, 13104).

Group 5: diabetes mellitus + curcumin (DC1).

Seven days after induction of experimental diabetes with STZ, 30 mg/kg curcumin was dissolved in corn oil and administered by intragastric gavage for 14 days.

Group 6: diabetes mellitus + curcumin (DC2).

Twenty-one days after induction of experimental diabetes with STZ, curcumin (30 mg/kg) was dissolved in corn oil and administered by intragastric gavage for 14 days.

Group 7: diabetes mellitus + curcumin (DC3).

Simultaneously with the injection of STZ to induce experimental diabetes, curcumin (30 mg/kg) was dissolved in corn oil and administered by intragastric gavage for 14 days.

The experimental diabetes model and blood glucose measurement

To induce the experimental diabetes model, a single dose of 50 mg/kg STZ (Cayman, 13,104) was dissolved in freshly prepared 0.1 M citrate buffer (pH 4.0) and administered intraperitoneally (i.p.) following overnight fasting (Kandemir et al. 2017). Access to feed was permitted after STZ injection (Andrade Cetto et al. 2000).

The experimental animals were given 5% glucose with drinking water to prevent hypoglycemia in the first 12–24 h after STZ injection. Seventy-two hours after STZ administration, blood samples collected from the tail veins of rats fasted overnight were dropped onto a glucometer (GI 300 Plus MED) strip to measure fasting blood glucose levels. Three measurements were taken from each animal, and those with a fasting blood glucose level of 250 mg/dL or above were considered diabetic and included in the study (Yuan et al. 2018). The control, sham, and curcumin groups received 0.1 M citrate buffer (pH 4.0) i.p.

Body weights and fasting blood glucose values of animals from all groups were measured at the beginning and end of the study. At the end of the experiment (35th day), blood samples were collected following the administration of 90/10 mg/kg ketamine (Ketasol, Richter Pharma, Wels, Austria) and xylazine (Citanest, AstraZeneca, Istanbul, Turkey) anesthesia.

Preparation of tissue samples

Perfusion and fixation

At the end of the experiment, on the 35th day, rats were sacrificed by cardiac perfusion method. For this, 0.9% saline was administered through a cannula from the left ventricular apex of the heart of the anesthetized rats. At the same time, the right atrium was cut, allowing the circulating blood to be removed and the physiological serum to be added to the circulation. When the blood was completely removed, a mixture of 4% paraformaldehyde + 2% glutaraldehyde was sent to the circulation through the cannula, and the tissues were fixed. After the perfusion process was completed, the bilateral ovary tissues were extracted, and the surrounding fat and connective tissues were trimmed. The dissected right ovaries were placed into jars containing 4% paraformaldehyde and 2% glutaraldehyde for stereological analysis. One of the left ovarian tissues was also set aside for electron microscopic examinations. The tissues obtained were subjected to a 1-week post-fixation process. Fixation solutions in the bottles were renewed every 3 days to enhance the fixation quality.

Body weight measurement and calculation of relative weight loss (%)

Relative weight loss percentages were calculated from the body weights measured at the beginning and end of the study.

Gonadosomatic index calculation (%)

The gonadosomatic index (GSI) measures the sexual maturity of animals. The GSI value in the present study was calculated using the formula (Walker et al. 2013)

$$GSI = \frac{GW}{BW} \bullet 100$$

where GW represents the sum of right and left ovary weights, and BW represents body weight.

Light microscopic procedures

After the post-fixation process, the right ovaries were placed into tissue processing cassettes for histological tissue examination. They were then washed for half a day to remove the fixation solution. In the dehydration phase, the tissues were passed through increasing graded alcohol series (70%, 80%, 96%, and 100%) and then cleared with xylene. Tissues were infiltrated and embedded with paraffin. Another individual enumerated each tissue from all experimental groups in order to perform a blind study during the tissue-labeling phase. The group names were not used during labeling. Sections 25 µm in thickness were from taken the right ovary tissue blocks using the systematic random sampling (SRS) method with a rotary microtome (Leica RM 2235, Vienna, Austria) for stereological analysis. The accuracy of the sampling interval was determined by means of a pilot study. The sections obtained were stained with hematoxylin and eosin (H&E) and made ready for analysis. Sections were examined with a light microscope (Olympus BX43, Center Valley, PA).

Electron microscopic procedures

Ovarian tissues from one animal from each group were embedded in resin blocks for electron microscopic analysis. Semi-thin sections (0.5 µm thickness) were cut using a rotary microtome (Leica RM 2135, Leica Instruments, Nussloch, Germany) and stained with toluidine blue. Semi-thin sections were examined using a light microscope (Olympus BX43, Center Valley, PA) and images were captured using a digital camera (Olympus SC50, Center Valley, PA) connected to the microscope with

lenses of 20×, 40×, and 100× magnification (N.A. 0.40; 0.65; 1.25 oil).

In addition, thin sections (70 nm) were taken from the same resin tissue blocks on cooper grids and stained with uranyl acetate, and lead citrate for electron microscopic observation. Thin sections were examined under an electron microscope (JEOL JSM-7001F, JEOL Ltd., Tokyo, Japan) and micrographs were taken.

Stereological analysis

In contrast to other quantitative techniques, stereological methods are design-based and unbiased methods based on statistical principles and stochastic geometric theory rather than assumptive-based approaches. The "optical fractionator method," one of the stereological methods, was therefore used to determine the numbers of follicles in the ovaries, while the "Cavalieri method" was employed for the volume parameter.

The optical fractionator method

To calculate the total number of follicles in the ovary, instead of evaluating all the sections obtained from the ovary in accordance with the "efficiency" principle of stereological methods, systematic random sampling (SRS) was performed at a ratio of 1:2 in the sections. The sampling rate of the sections to be selected for the study was determined by conducting a pilot study. Next, 25-µm-thick sample sections were taken from all blocks with 1:2 sampling in accordance with the SRS rule. For this process, after the first 25 µm section on the slide had been selected randomly, the other 25 µm sections were taken at 1:2 systematic intervals. Approximately 40 sampled sections were thus obtained from each tissue block.

The numbers of follicles in the sections were calculated using the optical fractionator probe in the computer-aided and special software stereology analysis system (Stereoinvestigator 9.0., MicroBrield Field; Colchester, USA) in the Recep Tayyip Erdoğan University Faculty of Medicine Department of Histology and Embryology. The parameters to be used in the study were determined by a pilot study (Table 1). During analysis, the morphological classification

Table 1 Counting parameters used in the optical fractionator method

Parameter	Value
Area of the counting frame (a)	6400 µm^2
Step size (X,Y)	40.000 µm^2
Area sampling fraction (asf)	6400 µm^2/40.000 µm^2
Disector height (h)	10 µm
Guard zone distance (upper)	3 µm

of ovarian follicles was based on the shape and number of layers of granulosa cells surrounding the oocyte (Myers et al. 2004).

After determining the appropriate parameters for counting, using the optical fractionator probe in the Stereo Investigator program (Stereo Investigator 9.0., MicroBrield Field; Colchester, USA), the boundaries of the area to be counted (the outer boundaries of the ovarian section) under the 1× objective lens were marked out. The size of the counting frame, the dissector height, and the numerical parameters were entered onto the relevant parts of the software and counted under a 63× objective lens. Follicle counting with the optical fractionator method was based on the presence or absence of the nucleus of the oocyte cell. Oocytes with a nucleolus were included in the count, while those without were excluded. The counting frame was systematically randomly placed on the sections along the determined step intervals using the Stereo Investigator software (Fig. 1a). To avoid affecting counting artifacts such as shrinkage and swelling that may occur in the cross-sections during histological procedures (sectioning, staining, etc.), counts were made at 10 µm depths after leaving a 3 µm safety margin from the upper surface of the section. The thickness of section was also measured at each probing site. Follicle counting was performed by applying the rules of the unbiased counting frame in the areas selected by means of the SRS. Oocyte nuclei falling into the count frame or intersecting the free edges of the frame were included in the count (Gundersen 1986) (Fig. 1b).

The total number of follicles "*N*" was calculated using the following formula:

$$N = \sum Q^- (1/ssf) \cdot (1/asf) \cdot (1/tsf)$$

According to the formula, the total number of follicles per ovary (**N**) was determined by multiplying the number of disector particles (number of oocyte nuclei) (ΣQ^-) counted after each volume during optical fractionator application and the fraction coefficients (sectional sampling fraction, ssf; area sampling fraction, asf; thickness sampling fraction, tsf).

Volume calculation using the Cavalieri method

Corpus luteum, vascular, connective tissue, cortex, medulla, preantral, and antral follicle volumes in the ovary sections were estimated using the Cavalieri principle, one of the unbiased stereological counting techniques. Calculation of the reference volume with this method is based on multiplying the total surface area (Σa_i) of the region of interest in the cross-sections by the section thickness (*t*). A "point" area measurement scale was used to find the surface area of the parameter of interest (corpus luteum, vascular, connective tissue, cortex, medulla, preantral, and antral follicle
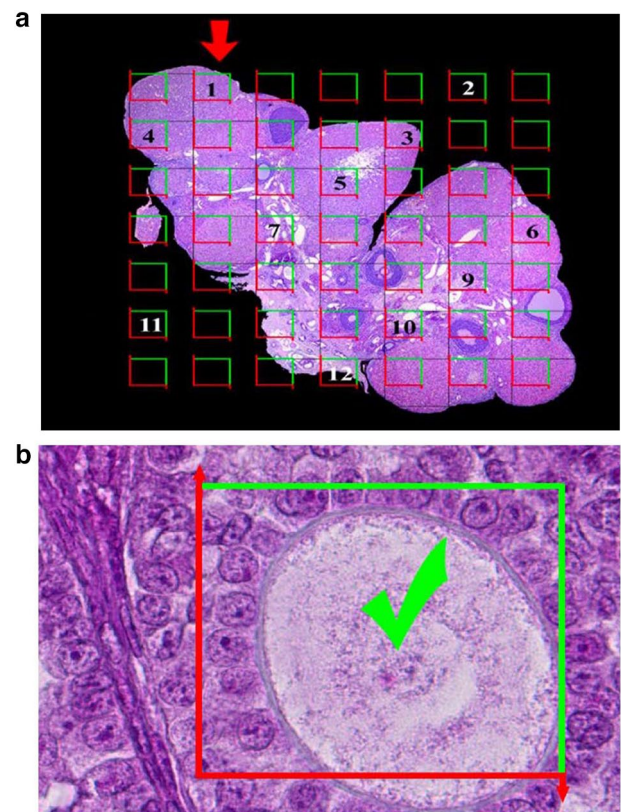
Fig. 1 While cell counting was performed with the optical fractionator counting method on the Stereo Investigator program, counting frames of a size determined in the pilot study (based on the determined step intervals and the SRS method) were placed over the cross-section images in the 1× lens (**a**). Application of the optical fractionator counting method. A countable nucleolus (falling into the counting frame or intersecting the free edges of the frame) can be seen in a sampling area selected by the SRS (**b**)

volumes) in the section. The point area measuring scale consists of systematic equidistant points in the form of a cross. The midpoint of each cross represents a point on the grid. Each of these points represents a unit scale area between the four points. Since the fixed distance between the points on the sections is known ($P_{(a)}$), if the point counting volume estimation grid is placed over a section image, it will intersect with as many points as the area represented by the relevant structure (ΣP_i). Multiplication of the total number of points superimposed on section (ΣP_i) by ($P_{(a)}$) yields the total area on that section (Gundersen 1986; Gundersen and Jensen 1987).
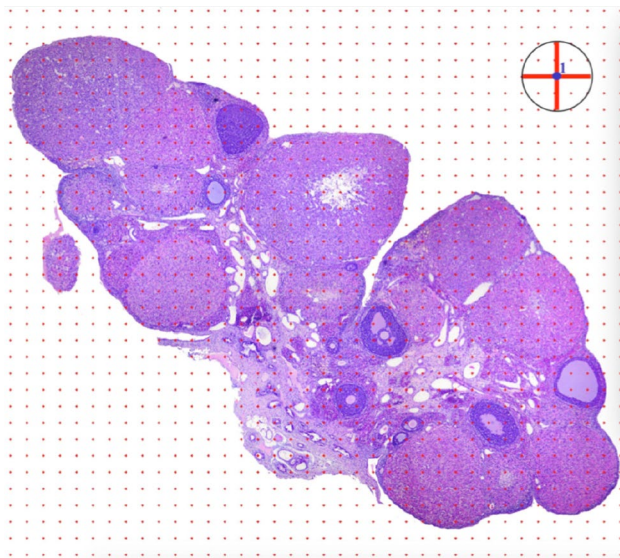
$$V_{ref} = \sum P_i \cdot t$$

$$P_i = P_{(a)}$$

In this formula, V_{ref} represents the total volume of the structure of interest, ΣP_i the total number of points

corresponding to the section projections, t the average section thickness, and $P_{(a)}$ the area represented by a point. Accordingly, sections were selected with a 1:4 resampling from the ovary sections selected by SRS, which were previously made at the rate of 1:2, and volume calculations were made in these sections. The images were then captured with 1:4 sampling on a 4× objective lens (Olympus BX43, Center Valley, PA) in the sample sections selected for calculating cortex and medulla volume. Following the pilot study, the area represented by a single point on the "point counting grid" was determined as 10,000 μm^2. A point counting volume estimation grid was placed over the cross-sectional images in Image J (Image Processing and Analysis in Java, NIH, USA) (Fig. 2). The cortex and medulla volumes were calculated by multiplying the number of points superimposing on the cortex and medulla by the section sampling rate, the area sampling rate, and the area represented by a point.

For calculating the volumes of the corpus luteum, blood vessels, connective tissue, and preantral and antral follicles, images of the same sections were taken with a 20× objective lens and using a 1/5 sampling rate. Following a pilot study, the area represented by a point on the test grid was determined as 9000 μm^2, and a point counting volume estimation grid was placed over the cross-sectional images in ImageJ (Image Processing and Analysis in Java, NIH, USA) program. The volumes were calculated by multiplying the number of points superimposing on the structures of interest by the section sampling rate, the area-sampling rate, and the area represented by a point.

Biochemical analysis

Biochemical analyses were performed at the Ondokuz Mayıs University Faculty of Medicine Department of Biochemistry. At the end of the experiment, but before perfusion, 1 mL blood samples were collected from the hearts of anesthetized rats and placed into EDTA tubes. The samples were then separated by centrifugation (Hettich, Tuttlingen, Germany) for 2000 rpm at 4 °C for 15 min. Serum samples were stored at −80 °C until investigation. CAT activity and SOD, FSH, and LH levels were measured in the serum samples.

Catalase enzyme activity analysis

A CAT assay kit (Cayman Chemical Company, USA) was used to compare antioxidant enzyme activities between the groups. The absorbent values of the serum samples were measured at 540 nm with a microplate reader (BioTek Synergy 4, BioTek Instruments Inc., Vermont, USA), and enzyme activity was expressed as μM protein.

Superoxide dismutase level analysis

An SOD ELISA kit (Bioassay Laboratory Technology, Shanghai, China cat. no. E0168Ra) was used to measure SOD levels. The amount of enzyme was measured at a 450 nm wavelength using a microplate absorbance reader (SunriseTM, Tecan Trading AG, Männedorf, Switzerland) and was calculated as ng/mL protein.

FSH and LH hormone level analysis

ELISA (Shanghai Sunred Biological Technology Co. Ltd, Shanghai, China) kits were used to measure FSH and LH levels in serum samples. FSH enzyme (IU/L) and LH (mIU/mL) concentrations were measured at 450 nm.

Histopathological evaluation

For histopathological examinations, left ovary tissues were fixed in glutaraldehyde solution (2%), and then divided into 1 mm^3 sections and washed with 0.1 M phosphate buffer. The second fixation was performed with osmium tetroxide (OsO_4) (1%) for 90 min. For resin tissue processing, following dehydration with graded alcohol series, tissues treated with propylene oxide were placed into araldite (an embedding medium suitable for thin sectioning), which was expected to infiltrate the tissues. The tissue particles were placed on the tip of the bullet-shaped molds, which

Fig. 2 When calculating the volume according to the Cavalieri method using the ImageJ program, the "point counting grid" consisting of equidistant points was placed over the ovary cross-section images by means of the software, and the points on the image of the structure whose volume was to be estimated were counted. The total surface area was estimated by multiplying the number of points obtained by the area represented by a point. The reference volume was determined by multiplying the total surface area of the region of interest in the cross-sections by the section thickness

were placed into an oven and allowed to harden at 55–60 °C (Tables 6 and 7). Semi-thin sections (0.5 µm) were taken from the prepared resin blocks with an ultramicrotome (Leica EM UC7, Vienna, Austria) and stained with toluidine blue. Images were captured using a microscope with a camera attachment (Olympus BX43, Center Valley, PA, USA) for histopathological examinations.

Statistical analysis

The numerical data obtained were subjected to statistical analysis using SPSS software (SPSS version 21.0; SPSS Inc., Chicago, IL, USA). The data were expressed as mean ± standard error. The Shapiro–Wilk test was used to test normality. For intergroup comparisons, data conforming to normal distribution were evaluated using the one-way ANOVA and Tukey tests. The Kruskal–Wallis and Tamhane tests were used to compare multiple groups not exhibiting normal distribution. $p < 0.05$ and $p < 0.01$ were considered statistically significant.

Results

Body weights

Relative weight loss (%) was calculated on the basis of the body weights measured at the beginning and end of the experiment. The relative weight loss in the DM group was higher than that in the control, DC2, and DC3 groups ($p < 0.05$), (Table 2).

Gonadosomatic index (GSI %)

The GSI in the DM group was significantly lower compared with the control, sham, and curcumin groups ($p < 0.01$). However, GSI values were significantly lower in the DC1, DC2, and DC3 groups compared with the DM group ($p < 0.01$) (Table 2).

Fasting blood glucose levels

Fasting blood glucose levels were higher in the DM group than in all the other groups ($p < 0.01$). Levels in the DC1, DC2, and DC3 groups were significantly lower than in the DM group ($p < 0.01$), (Table 2).

Table 2 Mean ± standard error of the mean (SEM) of relative weight loss (%), GSI (%), and blood glucose level (mg/dL)

	Control	Sham	Curcumin	DM	DC1	DC2	DC3
Relative weight loss (%)	**2.00 ± 2.10**[d]	7.49 ± 2.56	4.81 ± 6.03	**25.40 ± 8.41**[a,f,g]	15.00 ± 2.9	**4.33 ± 5.38**[d]	**1.55 ± 3.10**[d]
GSI (%)	**0.08 ± 0.005**[k]	**0.12 ± 0.007**[k]	**0.10 ± 0.006**[k]	**0.06 ± 0.003**[a,l,m,n]	**0.10 ± 0.001**[k]	**0.10 ± 0.005**[k]	**0.14 ± 0.005**[k]
Blood glucose level (mg/dL)	**94 ± 4.61**[k,l,m,n]	**152 ± 6.88**[k,l,m,n]	**130 ± 7.46**[k,l,m,n]	**488 ± 20.09**[h,i,j,k,l,m,n]	**308 ± 23.59**[h,i,j,k]	**340 ± 18.88**[h,i,j,k]	**317 ± 32.20**[h,i,j,k]

Significant differences in the comparison of groups are written in bold

[a]Different versus control ($p < 0.05$)

[b]Different versus sham ($p < 0.05$)

[c]Different versus curcumin ($p < 0.05$)

[d]Different versus DM ($p < 0.05$)

[e]Different versus DC1 ($p < 0.05$)

[f]Different versus DC2 ($p < 0.05$)

[g]Different versus DC3 ($p < 0.05$)

[h]Different versus control ($p < 0.01$)

[i]Different versus sham ($p < 0.01$)

[j]Different versus curcumin ($p < 0.01$)

[k]Different versus DM ($p < 0.01$)

[l]Different versus DC1 ($p < 0.01$)

[m]Different versus DC2

Stereological results

Primordial follicle number

The number of primordial follicles in the DM group decreased significantly compared with those in the control and DC2 groups ($p < 0.01$).

The number of primordial follicles in the DC1 group was significantly lower than in the control and DC2 groups ($p < 0.01$ and $p < 0.05$, respectively).

The number of primordial follicles in the DC2 group was significantly higher than in the DC3 group ($p < 0.01$). The number of primordial follicles in the control group was statistically significantly higher than in all the other groups ($p < 0.01$) (Table 3).

Preantral follicle numbers

A significant decrease was observed in the numbers of preantral follicles in the DM group compared with the control and sham groups ($p < 0.01$). However, no statistically significant difference was found between the DM, curcumin, DC1, DC2, and DC3 groups ($p \geq 0.05$).

The number of preantral follicles in the control group was significantly higher than in all the other groups ($p < 0.01$). The number of preantral follicles in the sham group was also

Table 3 Mean $\pm$ SEM of follicle number

	Control	Sham	Curcumin	DM	DC1	DC2	DC3
Primordial follicle number	$1648 \pm 100.903^{i,j,k,l,m,n}$	668.17 ± 71.342^{h}	539 ± 119.532^{h}	364.83 ± 36.257^{h}	406.83 ± 70.663^{h}	$891.33 \pm 75.575^{h,e,k,g}$	533.20 ± 59.008^{h}
CE	0.13	0.27	0.27	0.29	0.28	0.18	0.26
CV	0.13	0.23	0.77	0.22	0.38	0.18	0.22
Preantral follicle number	$1285.20 \pm 90.683^{j,k,l,m,n}$	1156.14 ± 155.43	765.17 ± 51.088^{h}	$412.67 \pm 23.57^{h,b}$	467.40 ± 82.844^{b}	$513.67 \pm 67.252^{b,h}$	784.60 ± 82.456^{h}
CE	0.15	0.2	0.22	0.26	0.29	0.24	0.21
CV	0.21	0.32	0.24	0.28	0.43	0.29	0.21
Antral follicle number	$362.50 \pm 11.63^{b,k,l,m,n}$	$214.83 \pm 24.33^{a,l}$	$254.00 \pm 22.97^{k,l}$	80.60 ± 7.04^{h}	$60.80 \pm 16.63^{h,k}$	$117.20 \pm 17.23^{h,k}$	$283.00 \pm 74.03^{h,k}$
CE	0.25	0.46	0.4	0.64	0.72	0.6	0.46
CV	0.07	0.28	0.41	0.36	0.61	0.45	0.73
Toplam follicle number	$3295.33 \pm 159.617^{i,j,k,l,m,n}$	2106.33 ± 196.538^{h}	$1558.67 \pm 124.488^{h,d,e}$	$858.33 \pm 53.672^{h,i,m,n}$	$935 \pm 132.210^{h,i,n}$	$1622.40 \pm 128.439^{h,l}$	$1600.80 \pm 86.224^{h,k,l}$
CE	0.09	0.14	0.15	0.18	0.19	0.14	0.15
CV	0.11	0.2	0.18	0.09	0.37	0.19	0.16

Significant differences in the comparison of groups are written in bold

[a] Different versus control ($p < 0.05$)

[b] Different versus sham ($p < 0.05$)

[c] Different versus curcumin ($p < 0.05$)

[d] Different versus DM ($p < 0.05$

[e] Different versus DC1 ($p < 0.05$)

[f] Different versus DC2 ($p < 0.05$)

[g] Different versus DC3 ($p < 0.05$)

[h] Different versus control ($p < 0.01$)

[i] Different versus sham ($p < 0.01$)

[j] Different versus curcumin ($p < 0.01$)

[k] Different versus DM ($p < 0.01$)

[l] Different versus DC1 ($p < 0.01$)

[m] Different versus DC2 ($p < 0.01$)

[n] Different versus DC3 ($p < 0.01$)

significantly higher compared with the DM, DC1, and DC2 groups ($p < 0.01$) (Table 3).

Antral follicle numbers

The number of antral follicles in the DM group was significantly lower than those in the control, curcumin, and DC3 groups ($p < 0.01$).

The number of antral follicles in the DC1 group was significantly lower than in the sham, curcumin, and DC3 groups ($p < 0.01$). Similarly, the DC2 group exhibited significantly fewer follicles than the DC3 group ($p < 0.01$). The number of antral follicles in the control group differed significantly from those in the other groups (except for the curcumin group) ($p < 0.01$) Table 3.

Total number of follicles

The total number of follicles in the DM group decreased significantly compared with the control, sham, and curcumin groups ($p < 0.01$). The total numbers of follicles in the DC2 and DC3 groups were also significantly higher than in the DM group ($p < 0.01$).

The total number of follicles in the DC1 group decreased significantly compared with the control, sham, curcumin, DC2, and DC3 groups ($p < 0.01$). In the control group, total follicle number was significantly higher than in all the other groups ($p < 0.01$) (Table 3).

Cavalieri volume estimation results

Preantral follicle volumes

The preantral follicle volume in the DM group was significantly lower than in the control and curcumin groups ($p < 0.01$).

The preantral follicle volume in the DC1 group decreased significantly compared with the control group ($p < 0.01$). A difference was observed between the DC2 group and the control and curcumin groups ($p < 0.05$), but not with the other groups ($p \geq 0.05$). A significant decrease was observed in the preantral follicle volume in the curcumin group compared with the control group ($p < 0.05$) (Table 4).

Antral follicle volumes

No statistically significant difference was observed between the groups in terms of antral follicle volumes ($p \geq 0.05$) (Table 4).

Corpus luteum volume

Corpus luteum volumes in the DM group decreased significantly compared with the control, sham, and curcumin groups ($p < 0.01$). In addition, while there was no significant difference between the DM group and the DC1 group ($p \geq 0.05$), the corpus luteum volume of the DM group was lower volume than in the DC2 and DC3 groups ($p < 0.01$). Similarly, the volume of the corpus luteum in the DC1 group was lower in than the control, curcumin, and DC3 groups ($p < 0.01$). The volume of the corpus luteum in the DC3 group was significantly lower than in the control group ($p < 0.01$). In addition, the corpus luteum volume in the sham group was significantly lower than that in the control group ($p < 0.01$), while the corpus luteum volume in the curcumin group was higher than that in the sham group ($p < 0.05$) (Table 4).

Connective tissue volumes

The connective tissue volume in the DM group increased significantly compared with the control and sham groups ($p < 0.01$). A significant decrease was observed in the DC1, DC2, and DC3 groups compared with the DM group ($p < 0.01$) (Table 4).

Blood vessel volumes

A decrease was determined in blood vessel volume in the DM group compared with the control, DC2, and DC3 groups ($p < 0.01$).

Also, a significant decrease was determined in the sham group compared with the control group ($p < 0.05$) (Table 4).

Cortex and medulla volumes

The cortex volumes in the DM and curcumin groups decreased significantly compared with the control group ($p < 0.05$). A significant decrease was also observed in the DC1 and DC2 groups compared with the control group ($p < 0.01$). Stereological analysis revealed no significant difference in medulla volumes in any of the study groups ($p \geq 0.05$) (Table 4).

Biochemical results

Catalase enzyme activity

A significant increase was observed in CAT activity in the DM group compared with the control, sham, curcumin, DC2, and DC3 groups ($p < 0.01$), but no significant difference was found with the DC1 group ($p \geq 0.05$). CAT activity

Table 4 Mean $\pm$ SEM of volumes

Group	Control	Sham	Curcumin	DM	DC1	DC2	DC3
Preantral follicle volume (mm^3)	**0.99 $\pm$ 0.11^{c,f}**	0.55 $\pm$ 0.10	**0.39 $\pm$ 0.03$^{a, f, k}$**	**0.12 $\pm$ 0.23^{h}**	**0.22 $\pm$ 0.04^{h}**	**0.22 $\pm$ 0.01^{a}**	0.46 $\pm$ 0.23
CE	0.02	0.03	0.04	0.06	0.05	0.05	0.04
CV	0.26	0.23	0.18	0.3	0.37	0.16	0.13
Antral follicle volume (mm^3)	0.79 $\pm$ 0.09	0.47 $\pm$ 0.07	0.39 $\pm$ 0.04	0.68 $\pm$ 0.04	0.59 $\pm$ 0.04	0.55 $\pm$ 0.05	0.72 $\pm$ 0.19
CE	0.03	0.03	0.03	0.04	0.03	0.03	0.03
CV	0.27	0.26	0.36	0.31	0.14	0.21	0.48
Corpus luteum volume (mm^3)	**8.10 $\pm$ 0.20^{i,k,l,n}**	**6.49 $\pm$ 0.17^{h}**	**7.61 $\pm$ 0.34^{b,k,l}**	**5.07 $\pm$ 0.15^{m},n**	**5.41 $\pm$ 0.31^{h},m,n**	**7.45 $\pm$ 0.49^{k},l**	**6.49 $\pm$ 0.21^{h}**
CE	0.01	0.02	0.01	0.01	0.01	0.02	0.01
CV	0.32	0.34	0.11	0.23	0.28	0.23	0.19
Connective tissue volume (mm^3)	**2.43 $\pm$ 0.34^{k}**	**1.74 $\pm$ 0.26^{k}**	**0.39 $\pm$ 0.03^{m}**	**3.38 $\pm$ 0.22^{h},i,l,m,n**	**2.26 $\pm$ 0.13^{k}**	**1.85 $\pm$ 0.03^{k}**	**1.73 $\pm$ 0.17^{k}**
CE	0.02	0.03	0.02	0.01	0.02	0.02	0.02
CV	0.3	0.4	0.2	0.15	0.09	0.05	0.16
Blood vessel volume (mm^3)	**1.42 $\pm$ 0.08^{b,k}**	**0.96 $\pm$ 0.04^{a}**	1.20 $\pm$ 0.10	**0.82 $\pm$ 0.04^{h},m,g**	1.20 $\pm$ 0.26	**1.28 $\pm$ 0.06^{k}**	**1.14 $\pm$ 0.04^{d}**
CE	0.02	0.09	0.02	0.02	0.03	0.02	0.03
CV	0.12	0.13	0.2	0.13	0.34	0.1	0.07
Ovarian cortex volume (mm^3)	**11.57 $\pm$ 0.35^{c,d,l,m}**	10.55 $\pm$ 1.07	**7.82 $\pm$ 0.69^{a}**	**7.87 $\pm$ 0.74^{a}**	**8.02 $\pm$ 0.42^{h}**	**7.95 $\pm$ 0.25^{h}**	8.77 $\pm$ 0.66
CE	0.01	0.02	0.01	0.01	0.01	0.01	0.02
CV	0.07	0.23	0.2	0.21	0.1	0.15	0.13
Ovarian medulla volume (mm^3)	3.08 $\pm$ 0.16	3.16 $\pm$ 0.39	1.97 $\pm$ 0.31	3.44 $\pm$ 0.52	2.06 $\pm$ 0.44	2.61 $\pm$ 0.31	3.64 $\pm$ 0.90
CE	0.01	0.01	0.02	0.02	0.02	0.02	0.02
CV	0.12	0.28	0.36	0.35	0.34	0.32	0.39

Significant differences in the comparison of groups are written in bold

[a]Different versus control ($p < 0.05$)

[b]Different versus sham ($p < 0.05$)

[c]Different versus curcumin ($p < 0.05$)

[d]Different versus DM ($p < 0.05$)

[e]Different versus DC1 ($p < 0.05$)

[f]Different versus DC2 ($p < 0.05$)

[g]Different versus DC3 ($p < 0.05$)

[h]Different versus control ($p < 0.01$)

[i]Different versus sham ($p < 0.01$)

[j]Different versus curcumin ($p < 0.01$)

[k]Different versus DM ($p < 0.01$)

[l]Different versus DC1 ($p < 0.01$)

[m]Different versus DC2 ($p < 0.01$)

[n]Different versus DC3 ($p < 0.01$)

in the DC1 group increased significantly compared with the control and DC3 groups ($p < 0.01$) (Table 5).

Superoxide dismutase levels

SOD enzyme levels in the DM group decreased significantly compared with all other groups ($p < 0.01$) (Table 5).

Table 5 Mean $\pm$ SEM of CAT activity (ng/mL), SOD level (ng/mL), FSH level (IU/L), and LH level (mIU/mL)

Group	Control	Sham	Curcumin	DM	DC1	DC2	DC3
CAT activity (ng/mL)	**130.30 ± 5.24[k],l**	**107.67 ± 16.50[k]**	**97.35 ± 18.74[k]**	**253.41 ± 7.11[h],i,j,m,n**	**180.83 ± 16.95[h],n**	**143.69 ± 15.94[k]**	**104.66 ± 4.31[k],l**
SOD level (ng/mL)	**4.11 ± 0.30[k]**	**3.89 ± 0.25[k]**	**3.60 ± 0.16[k]**	**1.84 ± 0.24[h],i,j,l,m,n**	3.31 ± 0.15	3.64 ± 0.14	3.57 ± 0.27
FSH level (IU/L)	12.01 ± 0.33	**10.61 ± 0.72[k],m**	**10.38 ± 1.16[k],m**	**6.07 ± 0.49[h],l,n**	**10.79 ± 0.51[k],m**	**6.39 ± 0.48[h],i,j,n**	**9.87 ± 0.68[k],m**
LH level (mIU/mL)	**33.06 ± 1.28[m]**	**35.68 ± 0.832[m]**	**34.40 ± 2.73[m]**	27.13 ± 3.27	28.08 ± 3.50	**21.29 ± 1.70[h],i,j**	30.59 ± 3.65

Significant differences in the comparison of groups are written in bold

[a]Different versus control ($p < 0.05$)

[b]Different versus sham ($p < 0.05$)

[c]Different versus curcumin ($p < 0.05$)

[d]Different versus DM ($p < 0.05$

[e]Different versus DC1 ($p < 0.05$)

[f]Different versus DC2 ($p < 0.05$)

[g]Different versus DC3 ($p < 0.05$)

[h]Different versus control ($p < 0.01$)

[i]Different versus sham ($p < 0.01$)

[j]Different versus curcumin ($p < 0.01$)

[k]Different versus DM ($p < 0.01$)

[l]Different versus DC1 ($p < 0.01$)

[m]Different versus DC2 ($p < 0.01$)

[n]Different versus DC3 ($p < 0.01$)

Serum FSH levels

FSH levels in the DM group decreased significantly compared with the control, sham, curcumin, DC1, and DC3 groups ($p < 0.01$). FSH levels in the DC2 and DC3 groups exhibited no significant difference from those of the control, sham, curcumin, or DC1 groups ($p \geq 0.05$).

FSH levels the DC1 group were significantly higher than in the DC2 group ($p < 0.01$). FSH levels in the DC2 group were significantly lower than in the control, sham, curcumin, and DC3 groups ($p < 0.01$), FSH levels the DC3 group were no different to those of the control, sham, or curcumin groups ($p \geq 0.05$) (Table 5).

Serum LH levels

LH levels in the DC2 group decreased significantly compared with the control, sham, and curcumin groups ($p < 0.01$) (Table 5).

Histopathological results

Examination of the general histological structure of the ovaries from the control group revealed a prominent single layer of cubic epithelium surrounding the outside of the ovary and the tunica albuginea layer rich in connective tissue fibers, together with multiple irregular cytoplasmic extensions on the apical surface of the epithelium (Fig. 3a). Oocytes surrounded by a single row of follicle cells with distinct borders were observed in the center of the primordial follicle, immediately below the ovarian epithelium (Fig. 3a). The preantral follicles in the cortex exhibited a normal appearance, the oocyte was located in the center, and these were surrounded by the zona pellucida and granulosa cells (Fig. 3b). The well-preserved oocyte in the center of the antral follicles from the control group, the surrounding zona pellucida, and the corona radiata cell layer surrounding it in a single line could all be easily distinguished. Follicular fluid filling the antrum surrounded the cumulus oophorus (Fig. 3c). The structure of the theca follicle surrounding the follicles was also well preserved (Fig. 3d). In the corpus luteum, numerous normal-appearing, large polygonal-shaped granulosa lutein cells with eosinophilic cytoplasm as well as surrounding theca lutein cells with well-preserved blood vessels were observed (Fig. 3e). The presence of a large number of blood vessels of different diameters with smooth borders and hilus cells could be seen within the loose connective tissue in the ovarian medulla in the different groups. Other structures in the medulla (connective tissue, blood, and lymph vessels) were well preserved (Fig. 3f).

Examination of the sections from the sham group revealed that the single-layer cubic cover epithelium covering the outer surface of the ovary, the tunica albuginea below the epithelium, and the follicles belonging to different stages of development in the ovarian cortex were all normal

Fig. 3 A single layer of cubic epithelium surrounding the outside of the ovary from the control group. The primordial follicle (**a**), preantral follicle (**b**), and antral follicle (**c**) can be seen. The border between the preantral follicle and the surrounding tissue is clear, and the theca follicle is well developed. A prominent zona pellucida surrounding the oocyte in the antral follicle, in which the antrum is filled with fluid, and the single-row arrangement of the surrounding corona radiata cells are particularly apparent. The theca follicle exhibited a distinct structure, together with a capillary network in the theca interna of the follicle, and the theca externa was rich in connective tissue fibers (**d**). The capillaries between the luteal cells in the structure of the corpus luteum and the cytoplasm of the luteal cells appear to be filled with secretory granules (**e**). Blood vessels and hilus cells (dashed lines) can be seen in the loose connective tissue (LCt), in which the blood vessels and connective tissue elements are normal in structure (**f**). *TF* theca follicle, *LC* luteal cells, *V* blood vessels, *GC* granulosa cells, *O* oocyte, *TF* theca follicle, *OE* ovarian epithelium, * mitosis in panel b, *ZP* zona pellucida, *Ant* antrum, *CR* corona radiata, *CO* cumulus oophorus. Bars: (**a, d, e**) 10 µm, (**b**) 20 µm, (**c**) 40 µm, (**d**) 50 µm
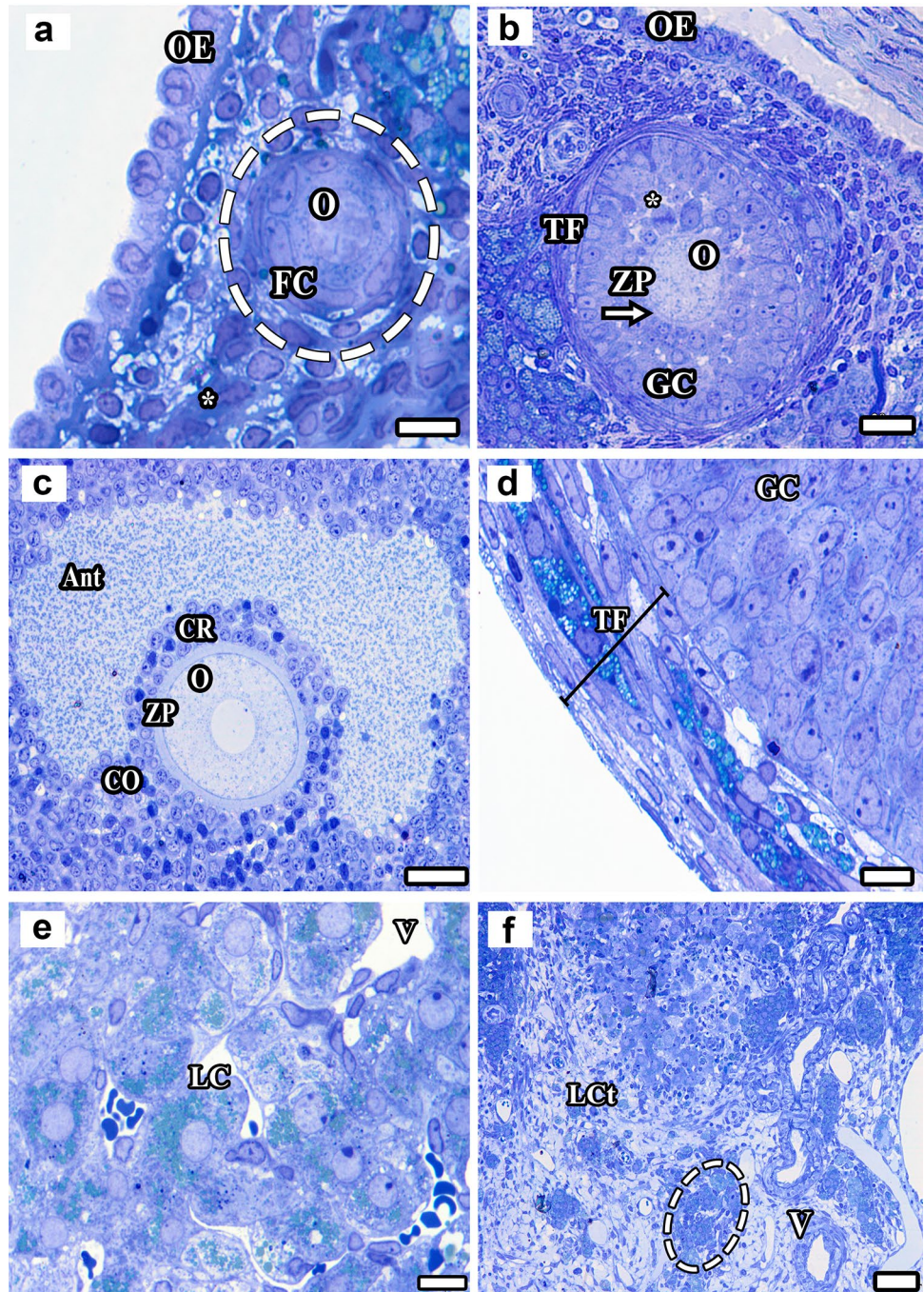

in appearance (Fig. 4a). Oocytes located on one side of the antrum and corona radiata cells lined up in a single row were observed in a Graafian follicle in sections from this group. Although no nucleus and nucleolus were observed in the structure of the oocyte, scattered chromatin filaments were a noteworthy finding (Fig. 4b). Granulosa lutein and theca lutein cells were distinguishable from one another in the corpus luteum, the cells of both layers exhibiting a normal appearance. The surrounding blood vessels were easily visible, and their lumen had a smooth border (Fig. 4c, d).

Lymph vessels with smooth lumen internal boundaries as well as clusters of cells resembling hilus cells were observed in the loose connective tissue in the medulla. The blood vessels were well protected, and their inner lumen boundaries were clear (Fig. 4e, f).

In the curcumin group ovaries, the cuboidal epithelial cells of the outside of the ovary were normal in appearance, with no microvilli-like extensions on their apical surfaces. Hollow structures were observed in the tunica albuginea, immediately below the epithelium (Fig. 5a). Distinct spaces

Fig. 4 Primordial follicles surrounded by single-layer flat follicle cells can be seen in the ovarian cortex from the sham group. The oocyte in the center of the primordial follicle and the surrounding flat-shaped follicular cells are normal in appearance (**a**). The zona pellucida is preserved in a Graafian follicle, although the granulosa cells surrounding the oocyte are discontinuous. The interna and externa layers of the theca follicle are well developed (**b**). Theca and granulosa lutein cells in the structure of the corpus luteum can be easily distinguished. The blood vessels around them are surrounded by a regular endothelium, and their lumen is open (**c**, **d**). Lymph capillaries and numerous blood vessels can be seen in the loose connective tissue of the medulla (**e**). There are numerous hilus cells, thought to be analogs of Leydig cells (**f**). *OE* ovarian epithelium, *TE* theca follicle, *GC* granulosa cells, *CR* corona radiata, *ZP* zona pellucida, *O* oocyte, *GLC* granulosa lutein cells, *TLC* theca lutein cells, *V* blood vein, *M* medulla, *HC* hilus cells, *Lv* lymph vessel. Bars: (**a**, **d**) 10 μm, (**b**) 40 μm, (**c**, **e**, **f**) 20 μm
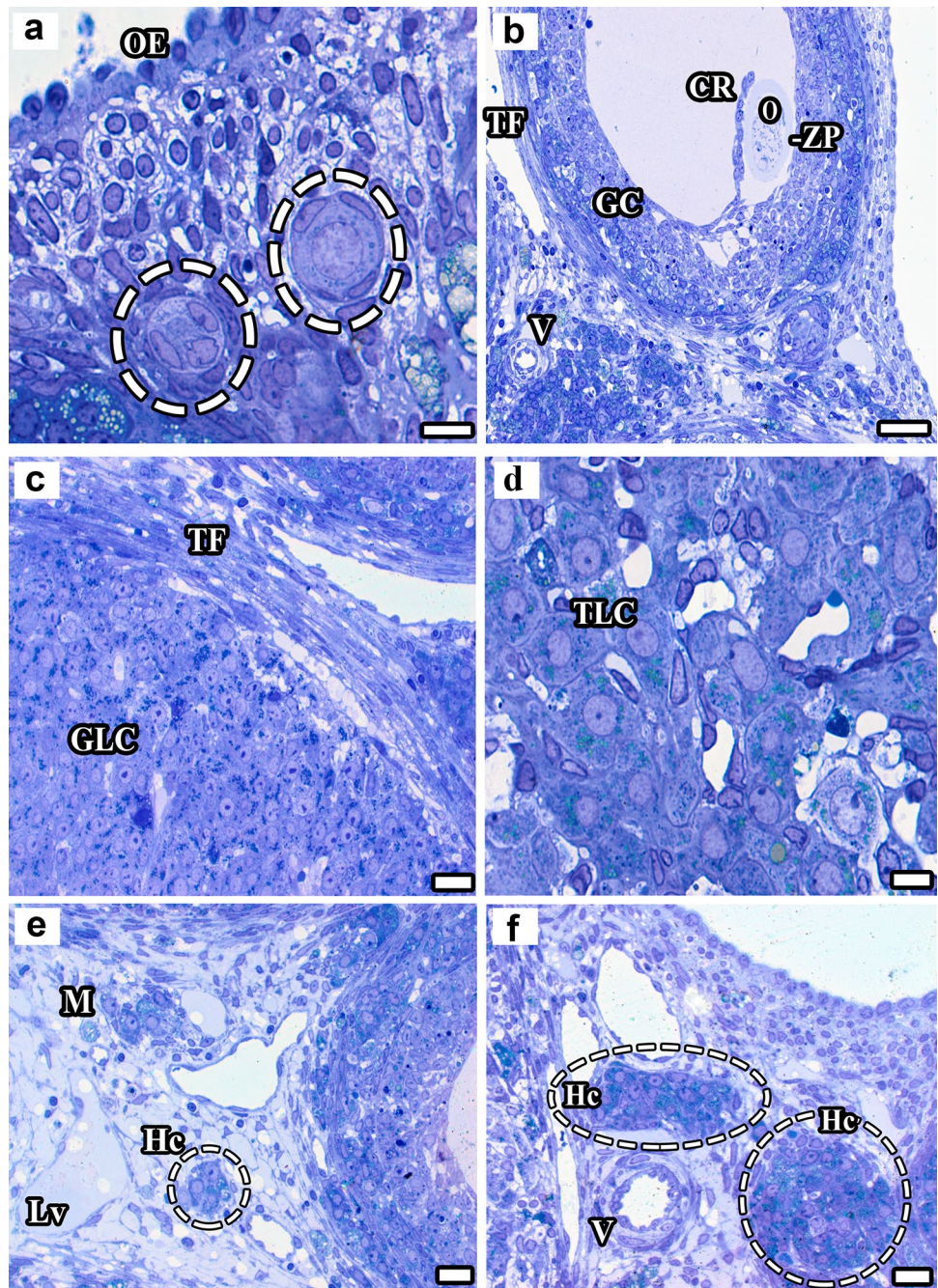

can be seen between luteal cells belonging to the corpus luteum. All elements of the luteal cells exhibited a normal structure (Fig. 5b). Evaluation of the relationship between theca follicle and granulosa cells showed that both theca follicle cells and granulosa cells exhibited a normal morphology. Some cells among the granulosa cells were apparently in the apoptotic process. There were cells around and inside the theca follicle, thought to be endocrine in character (Fig. 5c, d). Normally structured blood vessels and lymph capillaries were found in the loose connective tissue in the medulla. The presence of mast cells around the

blood vessels was noted (Fig. 5e). In the atretic follicle, the glassy membrane immediately after the granulosa cells was indistinct, and the theca follicle layer had lost its normal structure (Fig. 5f).

Single-layer epithelial cells of the ovaries from the DM group were cubic, flat, or prismatic, and had no uniform shape. The tunica albuginea beneath the epithelium consists of tightly arranged collagen fibers (Fig. 6a). The zona pellucida and the surrounding corona radiata cell layer were distinguishable in the Graafian follicle. The distance between the corona radiata cells was also greater. An increased

Fig. 5 A single-layered cubic ovary epithelium from the curcumin group, and the tunica albuginea immediately beneath. Note the presence of multiple shuttle-shaped fibroblasts in the connective tissue below the tunica albuginea (**a**). The capillaries are regular among the normal luteal cells in the corpus luteum (**b**). In terms of the relationship between the theca follicle and granulosa cells, the interna and externa layers of the theca follicle can be easily distinguished, and the distribution of capillaries in the theca interna is particularly striking. These capillaries, located close to the granulosa cells, provide the materials required by the granulosa cells. Numerous dark-shaped granulosa cells within the granulosa layer are thought to be cells undergoing apoptosis (**c**, **d**). Normal blood vessels can be seen in the loose connective tissue of the ovaries from the curcumin group. A large-diameter vessel thought to be a lymph vessel can be seen in the upper part of the artery with a thick wall (**e**). An atretic follicle and a well-preserved artery can be seen to the lower right of the follicle (**f**). *OE* ovarian epithelium, *TA* tunica albuginea, *LC* lutein cells, *TF* theca follicle, *GC* granulosa cells, *V* blood vessels, *MsC* mast cells, *Lv* lymph vessel, * degenerate where the oocyte is located. Bars: (**a, c, d**) 10 μm, (**b, f**) 20 μm, (**e**) 40 μm
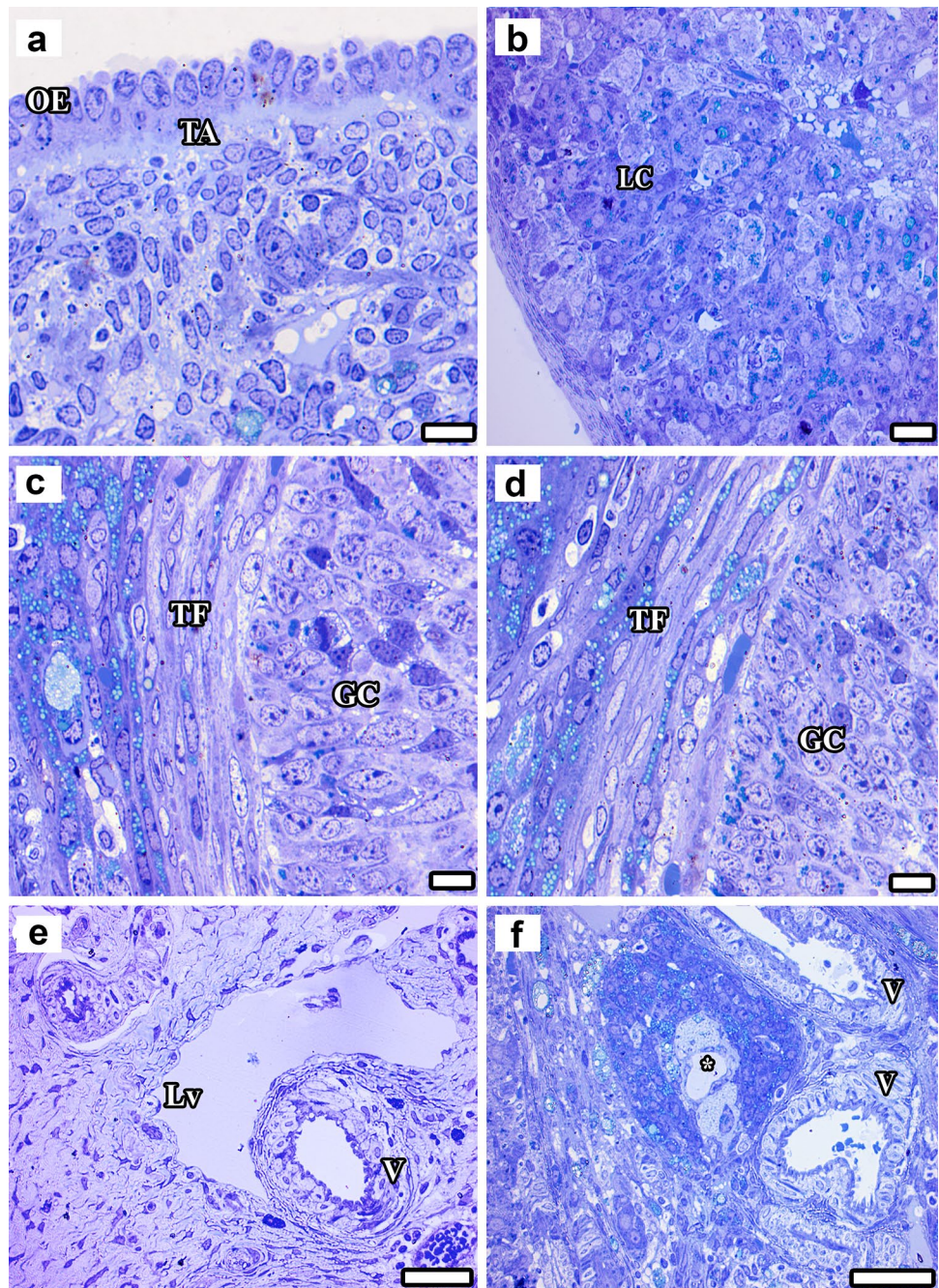

density of organelles and shrunken oocyte nucleus were observed in the oocyte cytoplasm (Fig. 6b). The integrity of the luteal cells of the corpus luteum that developed after ovulation was not preserved, and the distance between the cells had increased. This increased extracellular distance may provide increased capillary lumen diameters in the structure (Fig. 6c). In addition, the capillaries between the luteal cells, whose cell integrity was largely lost due to diabetes, were densely populated with erythrocyte clusters due to increased blood viscosity (Fig. 6d). Similarly, the blood vessel lumens in the structure of the ovary medulla, which

has loose connective tissue, were filled with an amorphous, reticular substance due to the increase in blood viscosity. Numerous irregular protrusions were seen on the surface of the endothelium facing the lumen. Cells known as hilus cells were observed in the medulla (Fig. 6e, f).

The ovary of DC1 group is covered by single-layered cuboidal cells in histological sections. Spaces were observed between epithelial cells, and their cytoplasm was stained darker. The tunica albuginea layer beneath the epithelium was not easily visible (Fig. 7a). The primary oocyte located in the center of the preantral follicle in the cortex
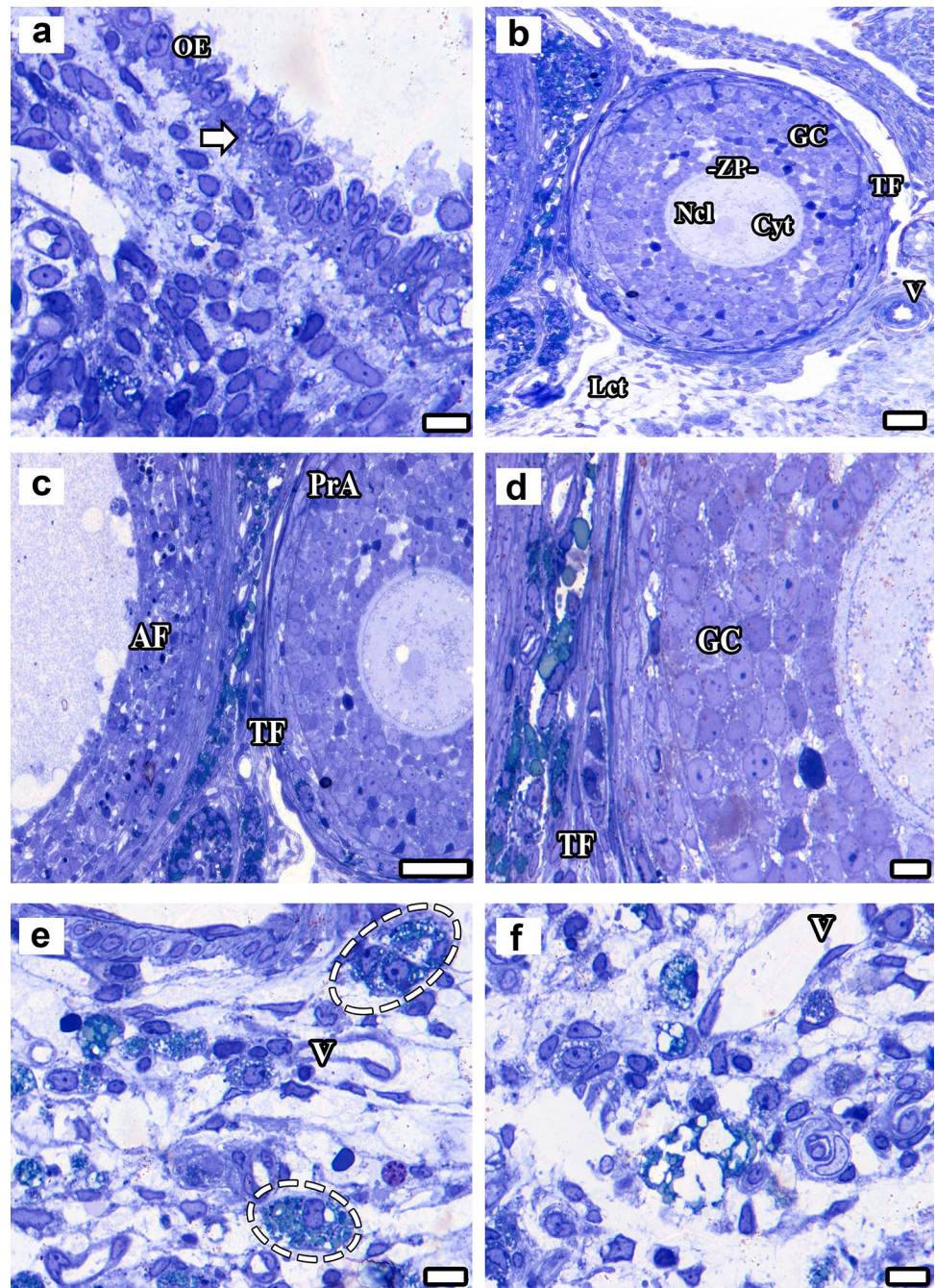
Fig. 6 The single-layer epithelial cells covering the surface of the ovaries from the DM group have no uniform shape. A thick tunica albuginea layer can be seen under the epithelial tissue. The epithelial cells lost their cubic shape in most places and were flat and prismatic in shape (**a**). The structure of a Graafian follicle shows numerous spaces between granulosa cells, which also have a densely stained cytoplasm and nucleus. The zona pellucida around the oocyte is partially thinned, the corona radiata cells are spaced apart, and the cells in this layer are of different sizes (**b**). The integrity of both luteal cells and capillaries in the corpus luteum is not well-preserved, and the distance between cells has increased (*). The cytoplasm of the luteal cells is denser, and the cell nuclei have shrunk (**c**, **d**). The medulla, which is filled with connective tissue in the form of loose connective tissue, contains blood vessels of different diameters. Both the inner and outer surfaces of the endothelial cells lining the inner face of the blood vessels lacked smooth borders. A significant quantity of an amorphous substance (a) can be seen in the lumens of blood vessels. *OE* ovarian epithelium, *TA* tunica albuginea, *ZP* zona pellucida, *Nuc* nucleus, *Cyt* cytoplasm, *Ant* antrum, *LC* luteal cells, *V* capillary, *Hc* irregular protrusions in the endothelium (arrow) hilus cells, *LCt* loose connective tissue. Bars: (**a, c–f**) 10 μm, (**b**) 20 μm
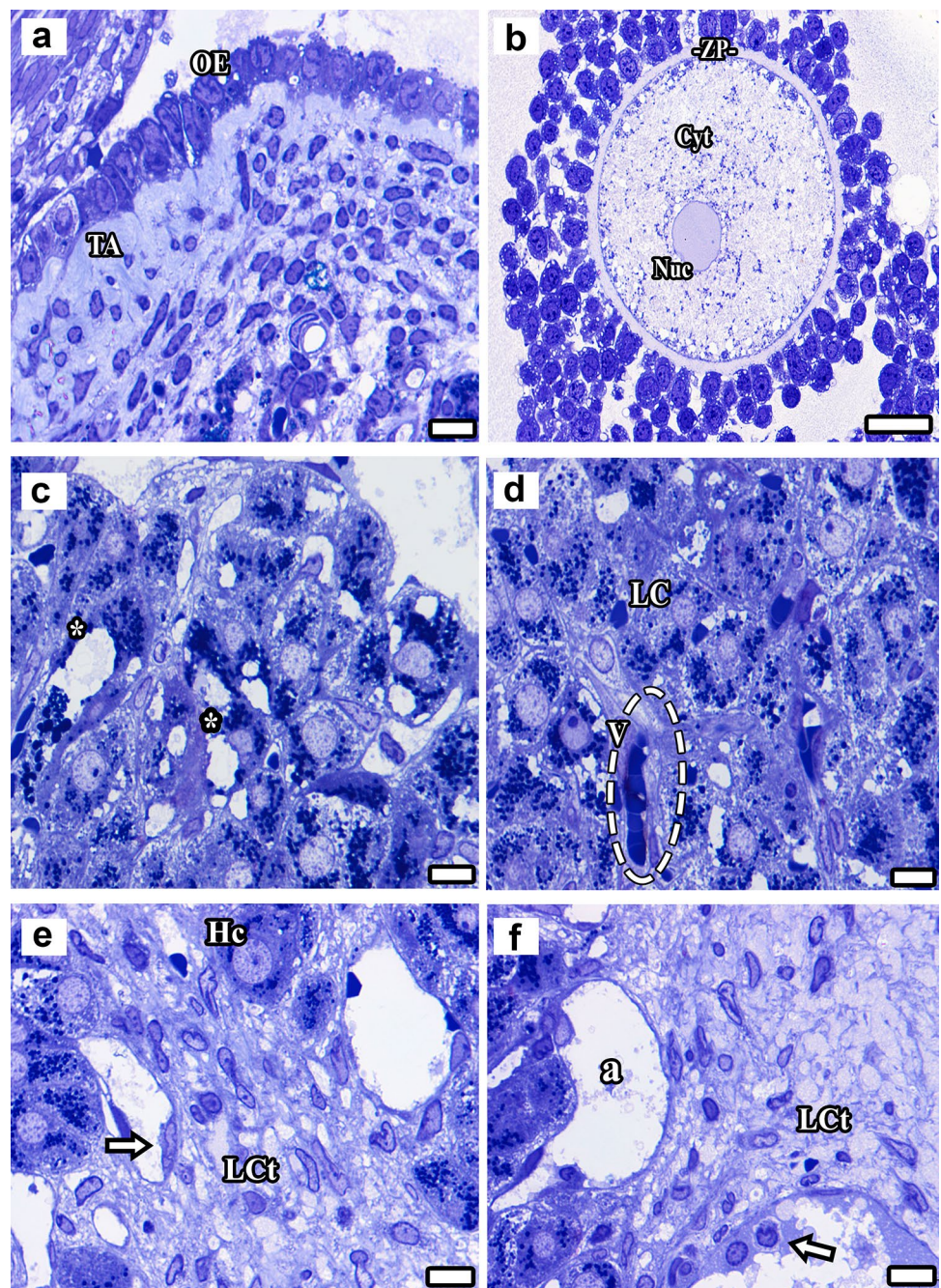
of the ovary was surrounded by a prominent zona pellucida. Although the nucleus membrane boundaries could not be easily distinguished, the nucleolus was very prominent. While granulosa cells surrounded by theca follicles mostly appeared normal, the labyrinth system between lutein cells was enlarged (Fig. 7b). The boundaries of the granulosa cells surrounding the antrum of the antral follicle in the cross section could not be easily distinguished, there were spaces between them, and they were surrounded by a theca follicle. The granulosa cells issued numerous irregular, microvillus-like cytoplasmic extensions towards the follicular fluid

(Fig. 7c). A basement membrane was observed between the theca follicle and granulosa cells, with a distinctive structure around the preantral follicles (Fig. 7d). The presence of numerous blood vessels of different diameters in the loose connective tissue in the ovarian medulla and hilus cells that synthesize androgens, regarded as analogs of Leydig cells in the testis, were seen (Fig. 7e). The oocyte in the lumen of the atretic follicle surrounded by loose connective tissue had disappeared, the space left being filled with tissue fluid (Fig. 7f).

Fig. 7 A single layer of cubic covering epithelium can be seen surrounding the ovary from the DC1 group. The spaces between the epithelial cells and their cell sizes different from one another (**a**). A preantral follicle structure in the cortex was well preserved, with boundaries easily distinguishable from the surrounding tissues. Small spaces formed between granulosa cells, and some cells had condensed into apoptosis (**b**). The boundaries of the granulosa cells surrounding the follicle antrum are not easily distinguished, there are spaces between them, and the granulosa cells are surrounded by a theca follicle (**c**). The basal membrane can be seen between the theca follicles and granulosa cells, with a distinctive structure around the preantral follicles. The internal and external layers of the theca follicle were well preserved (**d**). Numerous different types of cells can be seen in the loose connective tissue of the ovarian medulla (**e**, **f**). Arrow indicates dark-stained cytoplasm of epithelial cells. *OE* ovarian epithelium, *Ncl* nucleus, *GC* granulosa cells, *TF* theca follicle, *Cyt* cytoplasm, *ZP* zona pellucida, *AF* antral follicle, *PrA* preantral follicle, *LCt* loose connective tissue, dashed lines (hilus cells), *V* blood vessels of different diameters. Bars: (**a, d–f**) 10 μm, (**b**) 20 μm, (**c**) 40 μm


In the DC2 group, there were spaces between the single-layered cubic covering epithelium cells surrounding the ovary, and their cytoplasm were stained darker. The tunica albuginea layer under the epithelium was not clearly visible (Fig. 8a). A basement membrane was observed between the theca follicle and granulosa cells, with a distinctive structure around the preantral follicles (Fig. 8b). The internal and external layers of the theca follicle were well preserved. The corpus luteum cells, blood vessels, and the spaces between the cells all exhibited a normal appearance. The cytoplasm contents were well preserved, while most of the capillaries exhibited a normal structure, with an erythrocyte cluster appearing in the lumen of some (Fig. 8c, d). Loose connective tissue and rich blood vessels were seen in the ovarian medulla. Numerous lymph vessels, some with valves, were observed in addition to the blood vessels in the medulla (Fig. 8e). Examination of the structure of the atretic follicles revealed loss of the genus cell in the center. We think that degeneration of the follicle begins with the death of the oocyte. Collagen fibers were concentrated in the theca externa around the follicle, leading to atresia and the

Fig. 8 A single layer of cubic covering epithelium can be seen surrounding the ovary in the DC2 group. Spaces can be seen between the epithelial cells, and their cytoplasm is stained darker. The tunica albuginea layer below the epithelium exhibits a developed appearance (**a**). Prominent connective tissue can be seen around the theca externa of a preantral follicle, together with a glassy membrane (basement membrane) outside the granulosa cell layer (**b**). The cells, blood vessels, and intercellular spaces in the corpus luteum are normal in structure (**c, d**). Blood cells are clustered in the capillary lumen (dashed lines) (**d**). The ovary medulla is rich in loose connective tissue and blood vessels (**e**). The structure of an atretic follicle can be seen (**f**). *OE* ovarian epithelium, *TA* tunica albuginea, basement membrane (opposing arrowhead), *TF* theca follicle, *GC* granulosa cells, *ZP* zona pellucida, *Cyt* oocyte cytoplasm, *Nuc* oocyte nucleus, *CL* corpus luteum, *LC* luteal cells (LC), *V* blood vessel, *Lv* lymph vessel, *AF* antral follicle, *AtrF* atretic follicle. Bars: (**a, d**) 10 μm, (**b**) 20 μm, (**c, f**) 50 μm, (**e**) 100 μm
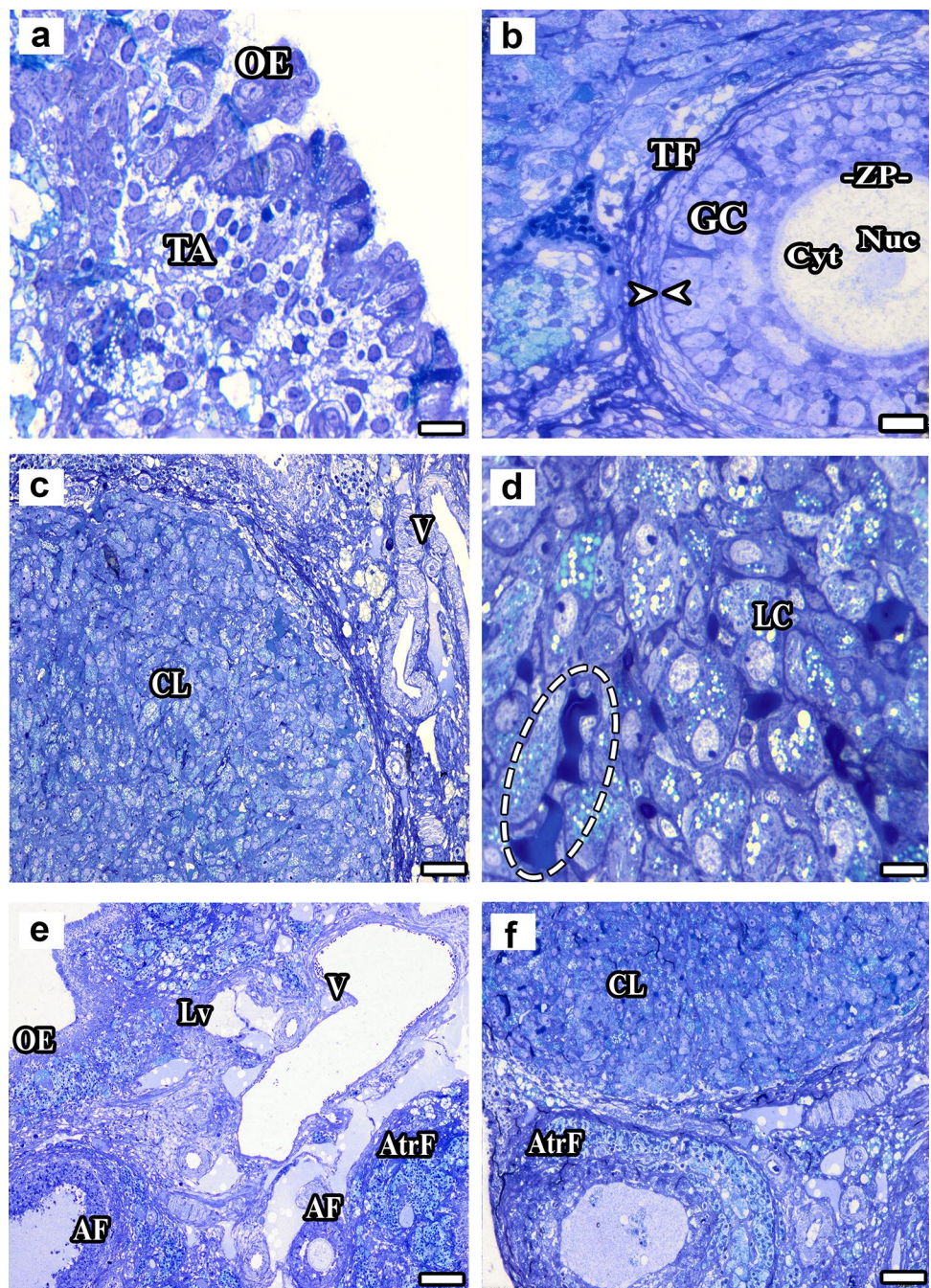

presence of numerous apoptotic cells in the granulosa cell layer (Fig. 8f).

Examination of the sections from the DC3 group ovaries revealed that the single-layered cubic covering epithelial cells surrounding the ovary surface were normal in appearance, with no microvillus-like protrusions on their apical faces. The presence of numerous hilus cells in the connective tissue was particularly noteworthy (Fig. 9a). In the antral follicles, the theca follicle surrounding the granulosa cells was clearly distinguished. Densely stained cells undergoing apoptosis were seen among the follicle cells (Fig. 9b).

The cells in the structure of the corpus luteum, blood vessels and the intercellular spaces were well preserved. The cytoplasm and nuclei of the lutein cells exhibited a normal appearance. Erythrocyte clustering was observed in the capillary lumen (Fig. 9c, d). The ovary medulla was filled with normal-appearing loose connective tissue and rich blood vessels. The presence of numerous irregular cytoplasmic extensions on the lumen facing surfaces of the endothelial cells lining the inner surface of the blood vessels was also noted (Fig. 9e, f).

Fig. 9 Image showing a single layer of cubic covering epithelium surrounding the surface of the DC3 group ovaries and the underlying tunica albuginea. The presence of a large number of hilus cells in the connective tissue is particularly remarkable (**a**). The extensively stained cells in the well-preserved antral follicle with a prominent theca follicle suggest that these cells are undergoing apoptosis. The zona pellucida was also well protected in this follicle (**b**). The structure of the corpus luteum was well protected. The cytoplasm and nuclei of the cells with endocrine characteristics were normal, and the lumen of the surrounding capillaries was open, with no erythrocyte clusters (**c, d**). The loose connective tissue in the normal ovarian medulla exhibited good organization and blood vessels of varying diameters. The lumen of the vessels in the medulla is open, and there are valves inside a lymph vessel (**e**). A large number of irregular cytoplasmic extensions (arrows) can be seen on the lumen-facing surface of the endothelial cells lining the inner surface of the blood vessels (**f**). *OE* ovarian epithelium, *TA* tunica albuginea, *V* blood vessel, *HC* hilus cells, *Ant* antrum, *ZP* zona pellucida, *O* oocyte, *GC* granulosa cells, *TF* theca follicle, *CL* corpus luteum, *LC* lutein cells, *V* blood vessels, *Lv* lymph vessels. Bars: (**a, b, d, f**) 10 μm, (**c**) 50 μm, (**e**) 100 μm
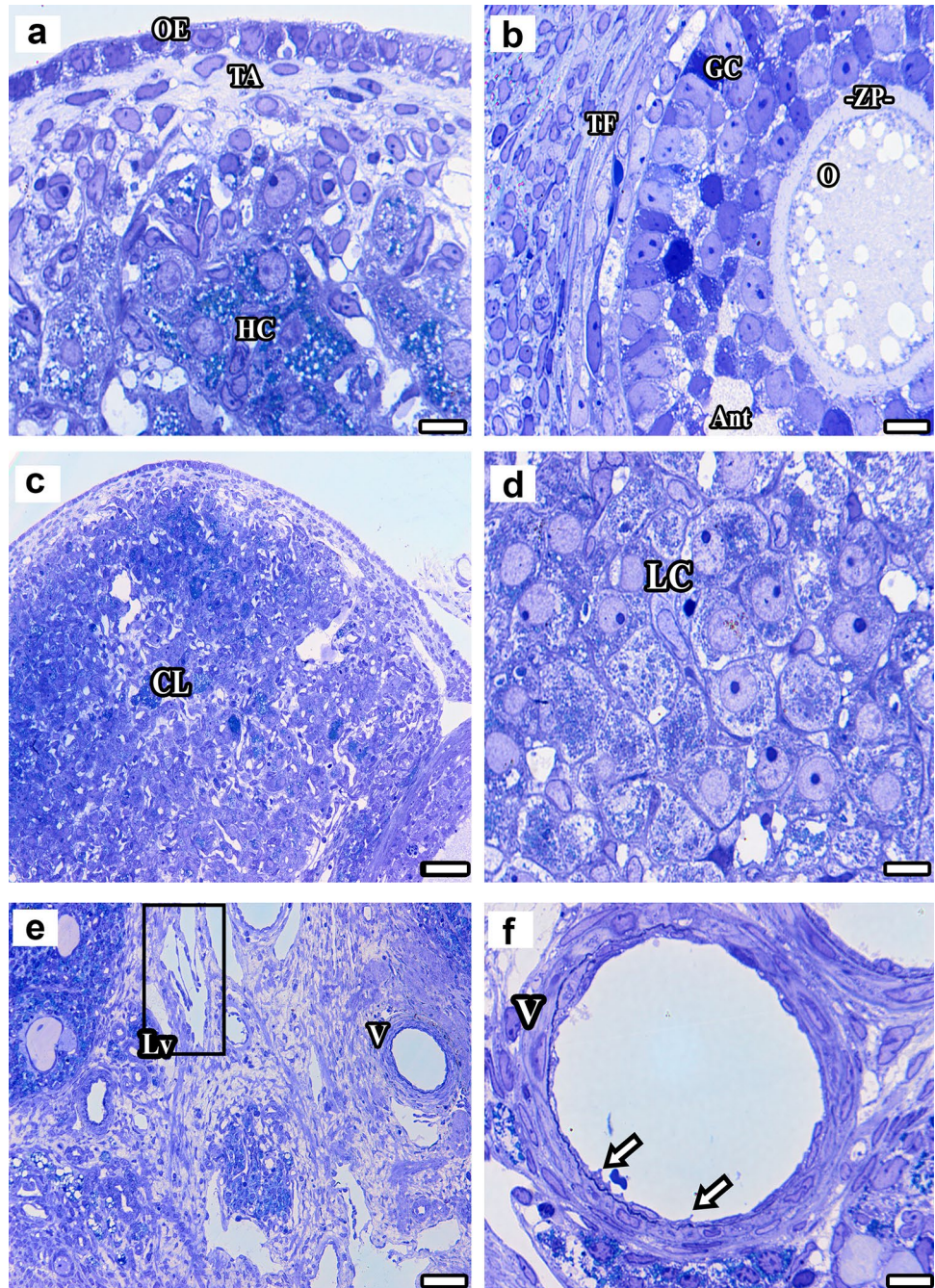
Electron microscopic results

When the fine structure of the ovaries of the control group is examined; it was observed that the interna and externa layers of the theca follicle were easily distinguished, and the follicle cells and the intercellular space had normal appearance (Fig. 10a). The presence of many cavities of different sizes between the cells in the granulosa layer of the DM group and the cells in the theca follicle layer attracted attention. Similar spaces were observed, especially in the cytoplasm of granulosa cells. Capillaries were observed between the theca follicle cells, the lumen of which was filled with a dense substance. Condensation of the cytoplasm and nuclei of some granulosa cells was noted, which is thought to have largely lost their function (Fig. 10b). It was observed that the structures forming the theca layer in the ovaries of the Sham group had a normal appearance and the structure of the cells was preserved (Fig. 10c). In the DC1 group, it was noticed that theca lutein cells were well preserved and the intercellular space was normal. Numerous lipid droplets were observed, with well-preserved well-defined nucleated granulosa cells (Fig. 10d). When the cytoplasm of granulosa
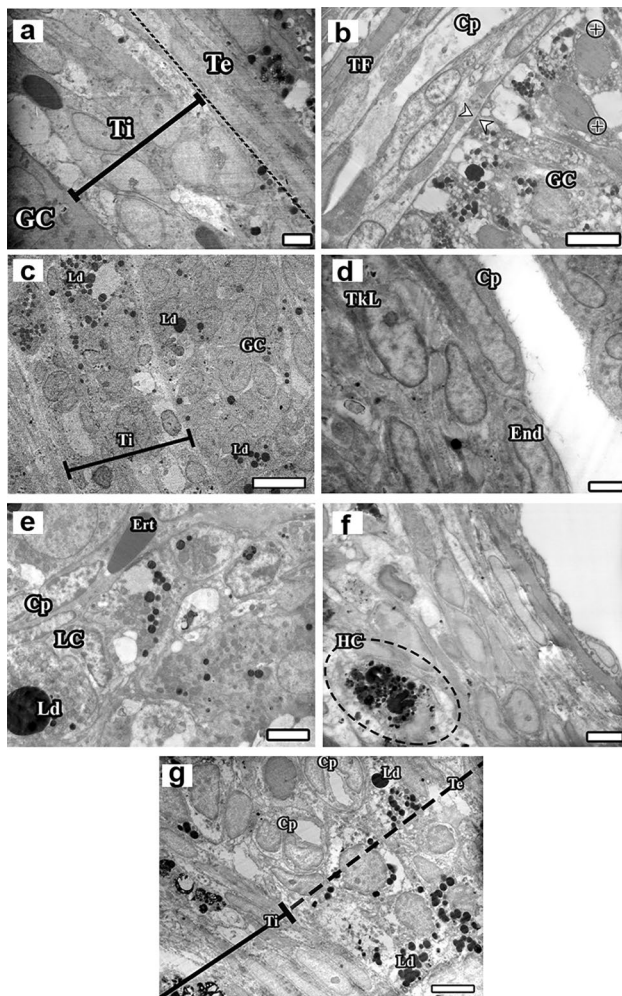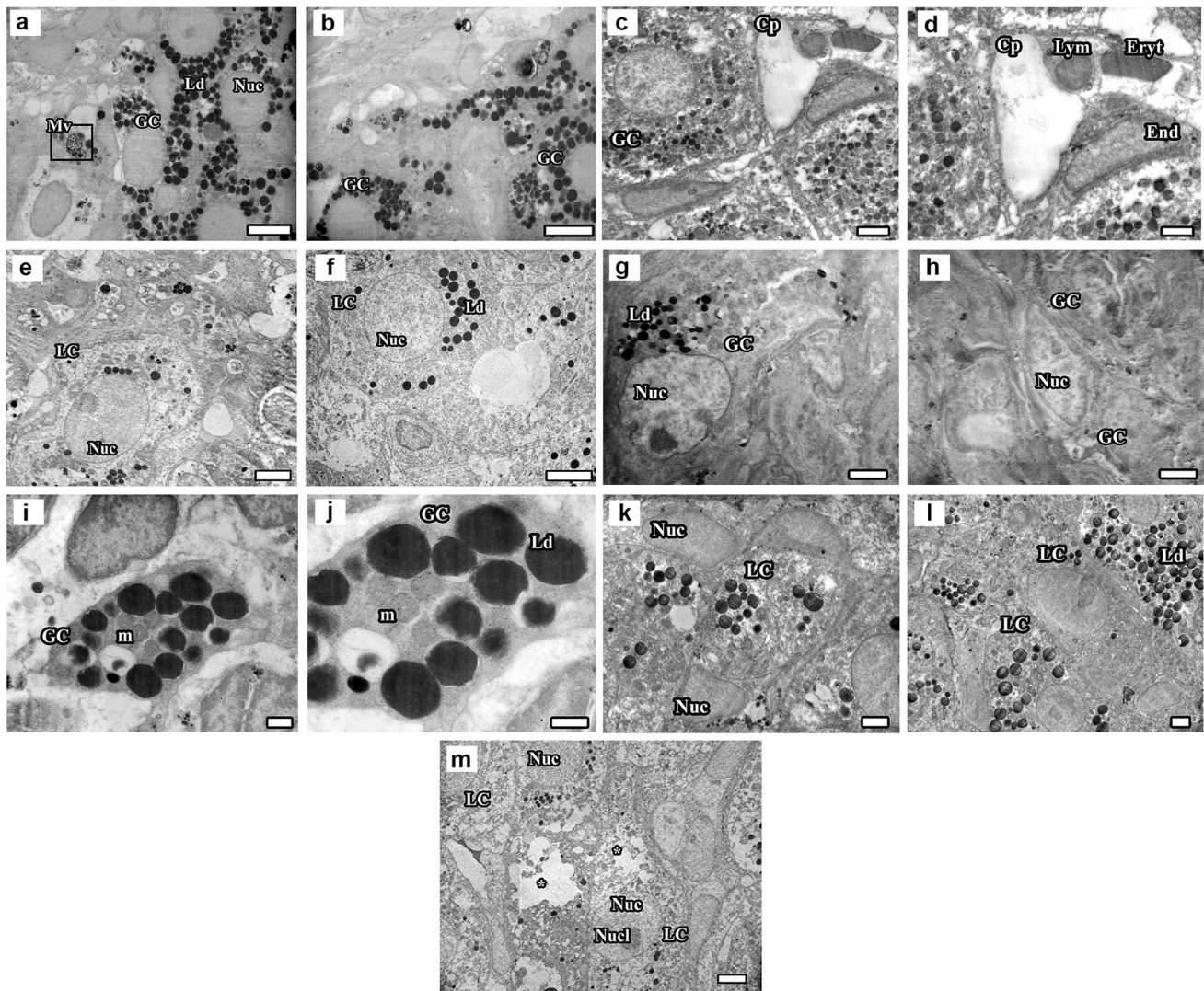
Fig. 10 In the control group, it is noticed that the theca follicle cells and the intercellular space appear normal and have a dense capillary network (**a**). In the DM group, it is noteworthy that there are many spaces of different sizes between the cells in the granulosum layer and the theca follicle layer. Capillaries located parallel to the cells of the theca follicle and filled with a dense lumen are observed. It is noteworthy that the cytoplasm and nuclei of some granulosum cells are concentrated (⊕), and it is thought that these cells have lost their functions to a large extent (**b**). In the sham group, theca interna cells and granulosum cells are normal. The lipid droplets in the theca and granulosum cells are seen (**c**). In the DC1 group, it is noticed that the endothelium of a capillary in the structure of the theca follicle has smooth borders, the surrounding lutein cells are well preserved, and the intercellular space is normal (**d**). When the cytoplasm of the cells in the follicle wall is examined in the image belonging to the curcumin group, it is noticed that lipid droplets, cell nuclei, and mitochondria are well preserved, and the intercellular space is in a normal structure (**e**). In DC2 group, luteal cell cytoplasm, nuclei, and intercellular spaces were observed to appear normal (**f**). In the DC3 group, it was noticed that theca externa cells and the intercellular space had a normal appearance. Nuclei and cytoplasm of lutein cells in the theca interna are well preserved, and the cells have many lipid droplets. It is observed that the capillary walls are smooth and the integrity of the vessel is preserved. The arrowheads indicate basal membrane. *Nuc* nucleus, *Ert* erythrocyte, *End* endothelium, *GC* granulosum cells, *HC* hilus cell, *LC* lutein cell, *TkL* theca lutein cell, *Cp* capillary, *Te* theca externa, *Ti* theca interna, *TF* theca follicle, *Ld* lipid droplet. Bars: (**a**) 3 μm, (**b**) 6 μm, (**c**) 10 μm, (**d**) 2 μm, (**e–g**) 4 μm

cells in the curcumin group was examined, it was observed that lipid droplets, cell nuclei, and mitochondria were well preserved, and the intercellular space was normal (Fig. 10e). In the DC2 group, luteal cell cytoplasm, nuclei, and intercellular spaces were observed to be normal. The lipid granules in the cell cytoplasm had smooth borders and the membranes surrounding the organelles were well preserved (Fig. 10f). In the DC3 group, the externa and interna layers of the theca follicle were easily distinguished. Theca externa cells and intercellular space were normal. It was observed that the nucleus and cytoplasm of the lutein cells in the theca interna were well preserved, and the cells had many lipid droplets (Fig. 10g).

It was noticed that the cytoplasm of the control group granulosa cells was filled with many lipid droplets. Well-developed capillaries were observed immediately after the basement membrane surrounding the granulosa cells. In addition, multivesicular structures were observed in some cells (Fig. 11a, b). On the contrary, the presence of numerous spaces between the granulosa cells and in the cell cytoplasm in the DM group was remarkable (Fig. 11c, d). It was observed that erythrocytes accumulated in the lumen of the capillaries between the granulosa cells. This may have occurred as a result of condensation of blood plasma. It was noticed that the cytoplasm and nucleus of the luteal cells in the sham group corpus luteum had normal structure and they contained many lipid droplets (Fig. 11e, f). It was observed that the cytoplasm of DC1 group granulosa cells, especially lipid droplets, nuclei, and nucleoli, had smooth borders. It was noticed that the intercellular space was normal (Fig. 11g, h). When the cytoplasm of curcumin group granulosa cells was examined, it was observed that lipid droplets, cell nuclei, and mitochondria were well preserved, and the intercellular space was normal (Fig. 11i, j). DC2 group lutein cells were well preserved, and the spacing between cells was normal (Fig. 11k, l). Although cavities were observed in the cytoplasm of some cells in the corpus luteum in the sections belonging to the DC3 group, it was noticed that the cell nucleus and nucleolus had a normal structure (Fig. 11m).

It was also observed that phagosomes with different sizes and densities in the cytoplasm of macrophages with different functional status, which are common in the medulla, in thin sections of ovaries belonging to all groups. It was noticed that the sizes of these macrophages, which are frequently encountered in the ovarian structure, also differ from each other (Fig. 12a–p).

A large number of normal blood vessels were noted in the ovarian sections of the control group. It was observed that the border between the endothelial cells lining the inner surface of the arterioles observed in the medulla was clear. The junctional complexes between the endothelium in the

Fig. 11 In the ovary of the control group, granulosa cells whose cytoplasm is filled with many dark lipid droplets and a multivesicular structure in the structure of a cell are observed (**a**, **b**). It is noteworthy that there are many spaces between the granulosa cells of the ovary belonging to the DM group and in the cell cytoplasm (**c**). A very large space is observed between the two granulosa cells located close to the capillaries (**c**, **d**). It is noticed that the cytoplasm and nucleus of the luteal cells in the corpus luteum in the ovaries belonging to the sham group have normal structure and many lipid droplets (**e**, **f**). In the ovary of the DC1 group, granulosa cells with lipid droplets are seen in its structure. It is observed that the cell structure and intercellular spacing are well preserved. The integrity of the nuclear membrane and the nucleolus with its clear border draw attention (**g**). The spacing between granulosa cells appears to be normal (**h**). It is noticed that the cells in the granulosa layer of the ovaries belonging to the curcumin group have a normal structure and their borders are clear. A granulosa cell filled with lipid droplets appears to have many mitochondria (**i**, **j**). Lutein cells with well-preserved nuclei, cytoplasm, and organelles are observed in the ovaries of the DC2 group (**k**, **l**). Although cavities are observed in the cytoplasm of some cells in the corpus luteum of the ovary belonging to the DC3 group, it is noticed that the cell nucleus and nucleolus have a normal structure (**m**). *Nuc* nucleus, *Nucl* nucleolus, * spaces in the cytoplasm, *Ld* lipid droplet, *LC* luteal cell, *GC* granulosa cell, *m* mitochondria, *End* endothelium, *Cp* capillary, *Mv* multivesicular structure, *Lym* lymphocyte. Bars: (**a**, **b**) 5 µm, (**c**–**e**, **g**, **m**) 3 µm, (**f**) 4 µm, (**h**, **k**, **l**) 2 µm, (**i**, **j**) 1 µm

arteriole wall and the prominent inner elastic membrane just below it, the smooth muscle cells surrounding it, and the endothelial cells were easily recognized (Fig. 13a, b). In the sections in the DM group, on the other hand, it was observed that the erythrocytes in the lumen of the capillaries in most areas adhered to the vessel wall (Fig. 13c, d). Similarly, in the sham group, erythrocytes in the capillary lumen were observed to pile up like a string of coins (Fig. 13e, f). It was noticed that extensive erythrocyte clusters were formed in the capillaries in DC1 and DC2 groups depending on the blood viscosity (Fig. 13g, h–k, l). Macrophages with a large number of phagosomes were observed in the ovarian
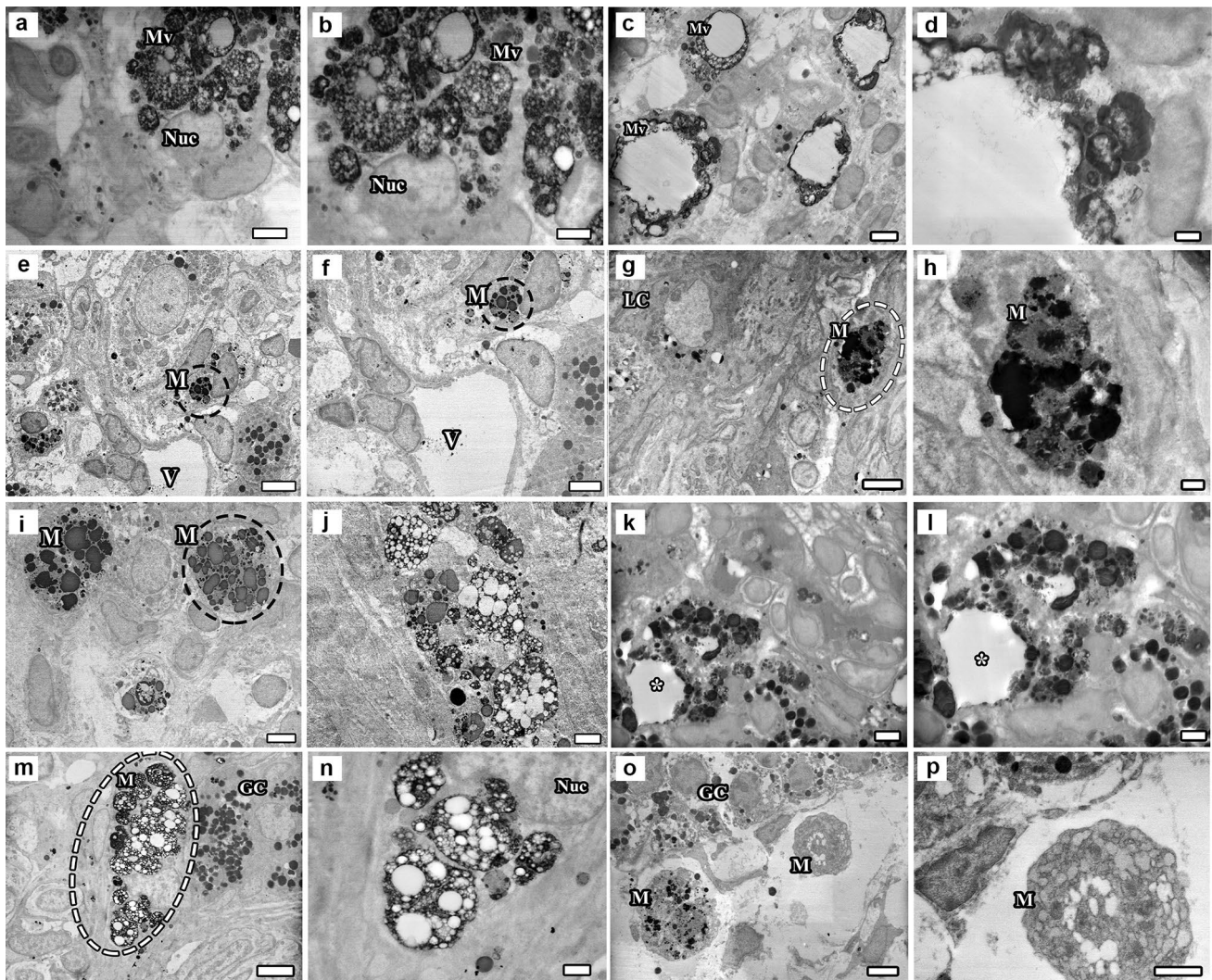
Fig. 12 Phagocytized structures of different sizes and densities are observed in the macrophage cytoplasm in the ovaries of the control group (**a**). A macrophage whose entire border cannot be observed has a large multivesicular structure in its cytoplasm (**b**). Macrophages with multivesicular structures of very different sizes are observed in the ovarian medulla of the DM group. The difference in size and density of multivesicular structures draws attention. The intermittent arrangement of connective tissue cells is noticeable (**c**, **d**). Macrophages, which are common in the ovarian medulla belonging to the sham group, are observed. Both sizes and densities of phagosomes taken into the cell cytoplasm can differ even within a cell (**e**, **f**, **i**, **j**). A macrophage located close to the corpus luteum is observed in the ovary of the DC1 group. There are phagosomes phagocytized in different sizes in the structure of the macrophage (**g**, **h**). In the structure of the ovary belonging to the DC2 group, a macrophage with indis-tinct borders and phagocytic structures of different sizes is observed. It is not known what the large diameter space (*) in the cytoplasm of the macrophage means (**k**, **l**). In the structure of the ovaries belonging to the curcumin group, a large-sized macrophage is seen with many vesicular-shaped phagosomes of different sizes in its cytoplasm. The granulosa cell, which contains many lipid droplets, is noticed (**m**, **n**). Macrophages, which are thought to be in two different functional states, located close to the granulosa cells, are observed in the ovaries of the DC3 group. While a large number of phagosomes of different sizes are seen in the structure of the macrophage on the left (**o**), it is noticed that the cytoplasm of the macrophage on the right is filled with many vacuoles (**p**). *GC* granulosa cell, *M* macrophage, *LC* luteal cell, *V* blood vessel, *Mv* multivesicular structure, *Nuc* nucleus. Bars: (**a**, **c**, **f**, **i**, **o**) 3 µm, (**b**, **l**, **p**) 2 µm, (**d**, **h**, **j**, **k**, **n**) 1 µm, (**e**) 5 µm, (**g**, **m**) 4 µm

medulla in the curcumin group. The cells in the connective tissue had smooth borders and normal nuclei (Fig. 13i, j). Heterochromatic nuclei and intensely stained cytoplasm, characteristic of granulosa cells, were striking. In addition, the capillary wall was smooth and vascular integrity was preserved (Fig. 13m, n).

Discussion

This study investigated the potential protective/healing effects of curcumin, an antidiabetic agent, on the ovary of in the early and late stages of diabetes (after 7 days and 21 days), and during the development of metabolic disorder
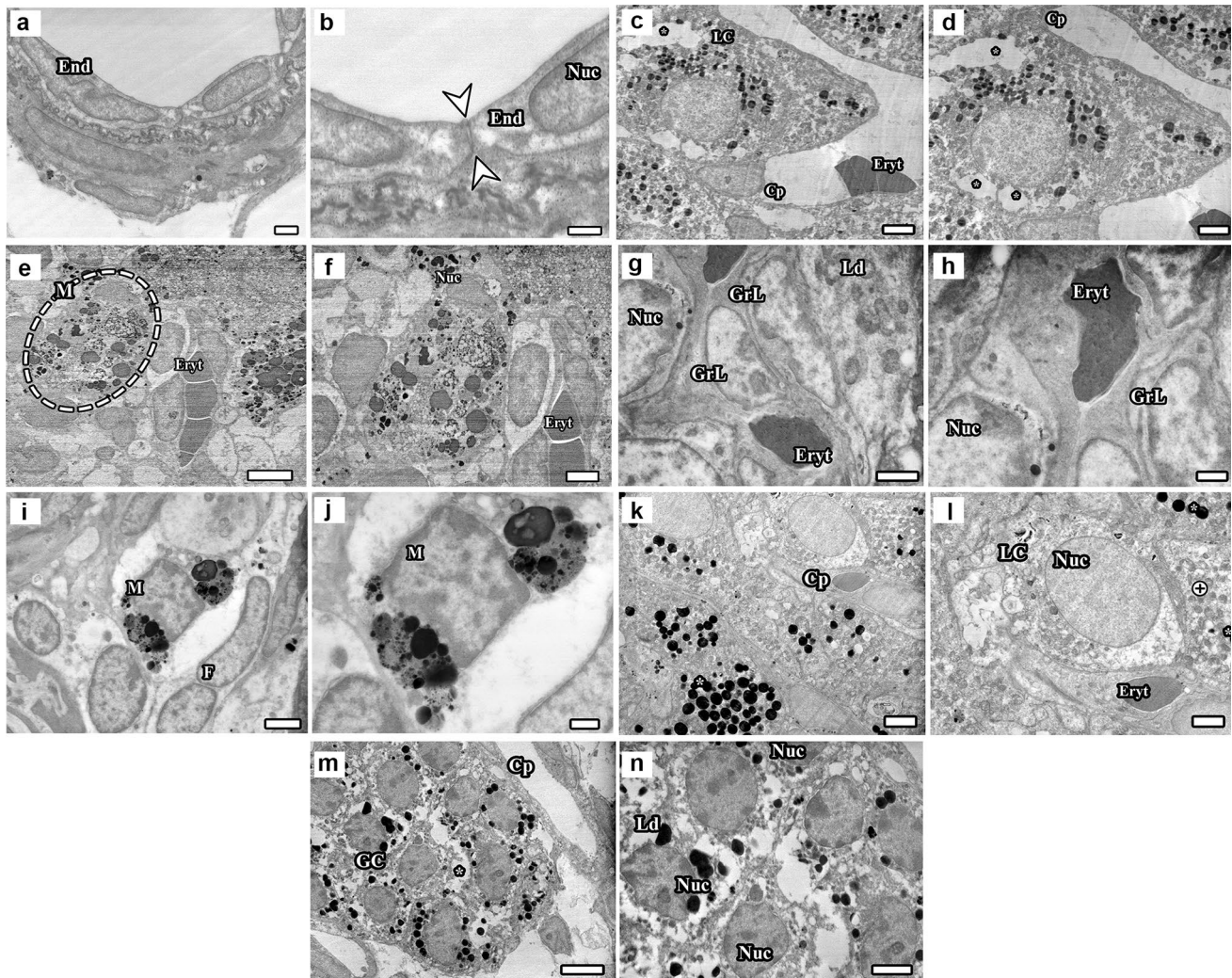
Fig. 13 An arteriole observed in normal structure in the ovarian medulla of the control group, the endothelium in the arteriole wall and the prominent inner elastic membrane and smooth muscle cell surrounding it are seen (**a**). The junctional complex (opposite arrows) between endothelial cells is discernible (**b**). It is noteworthy that there are spaces of different sizes in the cytoplasm of lutein cells located around the capillaries in a part of the corpus luteum in the ovary belonging to the DM group. It is noticed that the erythrocytes in the capillary lumen adhere to the vessel wall (**c, d**). Macrophages are frequently encountered in the ovary structure of the sham group (they vary in size). The macrophage observed in the picture can be given as an example of a very large cell. It is noteworthy that, in the capillary lumen, erythrocytes are stacked like a string of coins (**e, f**). Although normal granulosa lutein cells with well-preserved cell and nuclear borders are observed in the DC1 group, widespread erythrocyte clusters are noticed in the surrounding capillaries depending on the blood viscosity (**g, h**). A macrophage with a large number of phagosomes is observed in the ovarian medulla of the curcumin group. Connective tissue cells have smooth borders and have normal nuclei (**i, j**). Ovarian luteal cells are observed in the DC2 group. It is noticed that the cell cytoplasm, nuclei, and intercellular space appear normal. The lipid granules in the cell cytoplasm have smooth borders, and the membranes surrounding the organelles appear to be preserved (**k, l**). Since cells at different stages have different contents, they differ from each other with their dark and light staining characteristics [dark cell (*), light cell (⊕)]. There is an erythrocyte that completely fills the capillary lumen. Granulosum cells with a large number of lipid droplets are observed in the DC3 group. The spaces (*) between cells are remarkably wide. Heterochromatic nuclei are characteristic of intensely stained cytoplasm granulosum cells (**m, n**). *F* fibroblast, *M* macrophage, *L* lymphocyte, *Ert* erythrocyte, *Grl* granulosa lutein cell, *Cp* capillary, *GC* granulosum cells, *Nuc* nucleus, *Ld* lipid droplet, *LC* lutein cell, *End* endothelium. Bars: (**a, h, j, n**) 1 μm, (**b**) 0.5 μm, (**c, d, f, k**) 3 μm, (**e**) 5 μm, (**g, i, l**) 2 μm, (**m**) 4 μm

using stereological, biochemical, and histopathological methods. The results of our study show that diabetes has destructive effects on ovarian tissue by reducing the number and volume of follicles and disrupting the structure of the components of the ovarian tissue. Also, it has been found that curcumin exerts its protective effects on ovarian tissue by maintaining hormonal and antioxidant balance. In addition, curcumin was found to be more effective when used simultaneously with the development of diabetes.

Weight loss has frequently been described among the symptoms caused by hyperglycemia (Garris and Garris 2004; Kim et al. 2006; Ballester et al. 2007; Prasad et al. 2009). Similar findings were obtained in the present study. Type 1 DM generally results in a state of hypoleptinemia with mid- to long-term decreases in body weight. The adipose tissue hormone leptin participates in the integrated control of energy balance and reproductive activities. In this study, the excessive weight loss in DM group rats (excessive relative weight loss) and the pronounced lipid deficiency in ovarian stroma cells along with the progression of the disease suggest that abnormalities such as angiogenesis, secretion of steroid hormones, and impaired metabolism may be caused by adipose tissue deficiency. Curcumin has been reported to increase serum adiponectin and leptin levels in patients with metabolic syndrome (Panahi et al. 2016). One study stated that 15 mg/kg curcumin administration prevented body weight loss (El-Demerdash et al. 2009). Our study findings showed that treatment with curcumin at 30 mg/kg for 14 days 21 days after induction of diabetes (DC2) and concurrently with diabetes (DC3) had a positive effect on body weight maintenance. However, this effect was not observed in the group (DC1) given curcumin 7 days after induction of diabetes. This may be due to properties of curcumin such as suppressing preadipocyte differentiation in the early stages of diabetes and reducing both adipocyte numbers and fat content in adipose tissue (Ahn et al. 2010; Zhao et al. 2011).

The gonadosomatic index (GSI) in the DM group in this study decreased significantly compared with the control, sham, and curcumin groups. Studies involving diabetic rats have reported that abnormalities in the hypothalamic–pituitary–gonadal (HPG) axis (Valdes et al. 1991), and GnRH, which regulates sexual maturation and reproductive functions in mammals, cause faster shrinkage of the Graafian follicle, resulting in a decrease in ovarian mass and thus a decrease in GSI. In addition, GnRH exerts inhibitory effects on smaller follicles, and its sustained release may directly affect folliculogenesis, as well as causing a reduction in ovarian mass and GSI (Oluwatoyin et al. 2013). The decrease in folliculogenesis rate, follicle numbers, and FSH/LH levels in the present study suggest that the decrease in GSI in diabetic rats may have occurred as a result of a disruption of the HPG axis.

The GSI is an important criterion in evaluating the individual's reproductive potential. It increased significantly in the DC1, DC2, and DC3 groups compared with the DM group. No previous studies have shown the protective effect of curcumin on the GSI in diabetic rats. Our study is unique from that perspective. However, more comprehensive studies are now needed on this subject.

Examination of the fasting blood glucose levels of the experimental groups revealed a significant increase in the DM group compared with the control, sham, and curcumin groups. STZ is a widely used substance for experimental induction of DM in rats. A previous study reported that insulin secretion decreased and blood glucose levels increased as a result of the rapid depletion of pancreatic Langerhans islet β-cells in a DM group treated with STZ (Shima et al. 2011). Fasting blood glucose decreased significantly in the DC1, DC2, and DC3 groups in the present study compared with the DM group. However, curcumin administration did not reduce blood glucose level to those of the control, sham, and curcumin groups. Curcumin has been reported to reduce blood glucose levels in diabetic rats through regulation of the polyol pathway (Nabavi et al. 2015). The blood-glucose-lowering effect of curcumin has also been observed in human clinical studies of diabetic and prediabetic patients (Shafabakhsh et al. 2020). However, curcumin had no effect on blood glucose levels in individuals with normal levels at baseline. Further studies are now needed to evaluate the effects of curcumin on insulin resistance in diseases such as hyperglycemia and diabetes.

Stereological examination of the effects of diabetes on the ovary revealed a significant decrease in the numbers of primordial follicles in the DM group compared with the control group. Primordial follicle numbers increased significantly in the DC2 group compared with the DM group. Preantral follicle numbers decreased significantly in the DM group compared with the control and sham groups.

Antral follicle numbers in the DM group decreased significantly compared with the control and curcumin groups. When the protective effect of curcumin was analyzed in terms of antral follicle numbers, the number of follicles in the DC3 group increased significantly compared with the DM group. However, no difference was found between the DM group and the DC1 and DC2 groups. The number of antral follicles in the diabetes groups following curcumin administration was not as high as that in the control group, showing that curcumin was unable to normalize antral follicle numbers in the diabetes groups. Antral follicle numbers in the DC1 group decreased significantly compared with the sham group, but no difference was found between the DC2 and DC3 groups.

Total numbers of follicles in the DM group decreased significantly compared with the control, sham, and curcumin groups. The numbers of follicles in the DC2 and DC3 groups exhibited a significant increase compared with the DM group. No difference was observed between the DC1 group and the DM group. However, more follicles were observed in the control group than in the diabetes groups (DC1, DC2, and DC3), while no difference was found between the total number of follicles in the sham group and the number of follicles in the DC2 and DC3 groups.

Examination of follicular numbers can provide important information about the function of the ovary, especially the

relationship between folliculogenesis and the factors that regulate it (Myers et al. 2004). A reduction in the number of follicles in individuals with diabetes may lead to premature depletion of the follicle pool, leading to an increased risk of premature menopause and/or reduced fertility potential. Mouse, rat, and rabbit studies have investigated the effects of diabetes on the ovary (Tiwari-Pandey and Ram Sairam 2009; Farhad et al. 2013; Mehrabianfar et al. 2020).

In a study of Chinese hamsters, Garris (1984) found that different levels of hyperglycemic state (medium level 160–350 mg/dL blood glucose and high level 350 mg/dL blood glucose) caused severe adverse effects on ovarian functions. Total numbers of primary and secondary follicles in that study decreased in the diabetic group compared to the control group. As the hyperglycemic state progressed from moderate to high, the numbers of secondary follicles continued to decrease compared with the controls, and the percentage of available viable follicles dropped dramatically (Garris 1984). The results of our study, indicating a decrease in the numbers of preantral and antral (secondary) follicles in the DM group compared with the control group, are consistent with those of Garris. The number of antral follicles is considered one of the most important markers in evaluating functional ovarian reserves, in predicting the response to gonadotropin stimulation, and in predicting infertility and menopause risk (Depmann et al. 2016). Similarly, in Farhad et al.'s (2013) stereological mouse study, the numbers of preantral follicles and antral follicles decreased, while atretic follicle numbers increased, in the diabetic group compared with the control group. The authors also reported higher cortex and medulla volumes in the diabetic group compared with the control group. The authors suggested that this might be due to the formation of cortical vessels and polycystic structures. This finding differs from that of the present study, in which the cortex volume decreased significantly in the diabetic group compared with the control group. This decrease in cortex volume may be attributable to the decrease in blood vessel volume in the diabetic ovary, inflammation and increases in atretic follicles, and consequent slowing or pausing of folliculogenesis. Khedr (2016) reported that the numbers of primordial, primary, secondary, tertiary, and Graafian follicles in diabetic rat ovaries decreased significantly compared with the control group in a diabetes model induced with STZ. Researchers have reported that uncontrolled diabetes causes adverse biological effects by increasing oxidative stress and lipid peroxidation (Awadin et al. 2015). In that study, factors such as increased lipid peroxidation marker malondialdehyde (MDA) levels in the ovaries of diabetic rats, decreased SOD, CAT, and GPx activities, and decreased gonadotropins contributed to the degeneration of follicles (Khedr 2017).

No previous studies have investigated the effects of curcumin on the diabetic ovary, although it has been reported to protect mouse, rat, and rabbit ovary cells from pro-apoptotic, pronecrotic, and antiproliferative effects in the face of various oxidative stress factors (Tiwari-Pandey and Ram Sairam 2009). Curcumin has frequently been shown to exhibit different effects under varying stress conditions (Tiwari-Pandey and Ram Sairam 2009; Aktas et al. 2012; Sak et al. 2013). Despite the known widespread antioxidant effects of curcumin, the data obtained from the group (DC1) in which this substance was administered 7 days after diabetes induction in the present study confirmed that curcumin might exhibit different effects on organs and tissues under varying stress conditions. To summarize, curcumin was protective against diabetes in the DC2 and DC3 groups due to its antioxidant properties, while it exhibited no protective properties in the DC1 group.

Although the antioxidant properties of curcumin have been proven by numerous studies, it should be remembered that it cannot completely eliminate ROS, and that its anti-inflammatory and anti-apoptotic activities may be affected by numerous factors (Ferguson et al. 2021; Memarzia et al. 2021). In addition, the apoptotic process can be triggered by the Fas/FasL pathway, as well as by various signals and pathways (Wang and Su 2018). The occurrence of follicular imbalances due to hyperglycemia in the early stages of DM suggests that the antioxidant activity of curcumin is insufficient to eliminate or reduce these adverse effects caused by diabetes. The excessively increased oxidative stress and hyperglycemia that occur in the cells in the chronic period with the induction of DM may have masked the protective role of curcumin in the follicles and the general structure of the ovary. This may be due to the production of antioxidant-induced stress by disturbing the balance between antioxidants and increased reactive species.

Primordial follicles are the follicles most resistant to external factors. However, preantral follicles can easily progress to apoptosis by being more affected by environmental conditions. The reason why curcumin does not exert a protective effect on preantral follicle numbers in diabetic groups treated with curcumin is that the developing follicles are more sensitive to external factors due to their structure, at this stage. Diabetes causes a severe deterioration in the follicle, and the dose of curcumin applied may not be sufficiently strong to restore the structure.

The mechanisms by which the primordial follicles are protected and the principal mechanisms responsible for the loss of preantral and antral follicles at different stages of diabetes have recently emerged as a new research topic. The results of the present study show a pro-oxidant effect on primordial, preantral and antral follicle numbers when curcumin was administered days after the development of diabetes. However, when administered simultaneously with the development of diabetes, it affected only the antral follicles. When given 21 days after the development of diabetes,

it exhibited an antioxidant effect on and protected primordial follicle numbers. Histopathological examinations at the level of light and electron microscopy showed that curcumin exhibits protective effects on the structural and functional components of the diabetic ovary. In the curcumin-treated groups, the connective tissue and blood vessels were relatively well protected, the theca follicle around the follicles exhibited a clear organization, the structure of the glassy membrane (basement membrane) was preserved, and the internal and external layers of the theca follicle were easily visible. In the diabetic groups treated with curcumin, collagen fiber density/organization in the theca externa layer and the capillary network in the interna layer was smooth and rich. The structure of the zona pellucida was also preserved in these groups, the corpus luteum cells, blood vessels, and the spaces between the cells exhibited a normal appearance, and the luteal cell contents were also well preserved.

Ovarian follicular volume is the best indicator of follicular growth (Yavas and Selub 2009). In the present study, ovarian follicle volumes were estimated using the Cavalieri volume estimation method. The preantral follicle volume in the DM group exhibited an extreme decrease compared with the control and curcumin groups. No difference was observed in preantral follicle volumes between the sham and the DM groups. No difference was determined between the DC1, DC2, and DC3 groups treated with curcumin in terms of preantral follicle volume and the DM group. Finally, no difference was observed between the DM group and the other groups.

In a study using acute and chronic insulin-dependent diabetes models, the authors reported that pre-ovulatory oocytes were significantly smaller in size compared with the control group in both models, and that the developing follicles were smaller in size and contained more apoptotic foci (Chang et al. 2005). In addition, similarly to follicle sizes, the numbers of pre-ovulatory oocytes and corpus luteum decreased in hyperglycemic Akita mice compared with control animals (Chang et al. 2005). Researchers have suggested that abnormally low insulin, which acts as a paracrine factor to facilitate the transition from the primordial follicle to the primary follicle, may inhibit or delay follicle transitions (Kezele et al. 2002). In another study, evaluating the protective effect of *Aloe vera*, a plant with hypoglycemic effects, on the rat ovarian structure, the researchers found a significant reduction in secondary and tertiary follicle diameters in diabetic rats in the group with experimental diabetes induced by STZ (Shima et al. 2011). The fact that the preantral follicle volumes obtained from our stereological analysis were lower in the diabetic group compared with the control group is consistent with those studies.

Another study examining the effects of maternal diabetes reported decreased numbers and diameters of primary and preantral follicles decreased in the ovaries of offspring born to diabetic mothers (Khaksar et al. 2013). Similarly, Tatewaki et al. (1989) observed that the percentage of primary follicles, secondary follicles, and tertiary follicles decreased in diabetic mice compared with the control group, while the percentage of atretic follicles increased. Mehrabianfar et al. (2020) also reported that weight and volume of ovary is reduced in diabetic animals (Mehrabianfar et al. 2020). According to our findings, the decrease in the preantral follicle volume in the DM group may be due to the decrease in androgen production in follicle theca cells and changes in estrogen biosynthesis. This is because the gradual increase in estrogen production correlates with the increase in follicular surface area. In other words, three-dimensional follicular growth occurs as a result of the proliferation of theca interna and externa cells on the surface of the follicle. In addition, FSH/LH levels impaired due to diabetes may reduce the amount of estrogen released from follicular cells (Ballester et al. 2007). The absence of any difference in antral follicle volume between the groups in the present study may be due the heterogeneity of the data in the groups, due to the fact that the follicle has a large volume and/or that the coefficients of variation of the groups are high.

Dietary curcumin in rabbits has been found to increase the diameters of primary, secondary and tertiary follicles (Sirotkin et al. 2017). The absence of any difference between the diabetic group (DM) and other groups DC1, DC2, and DC3, treated with curcumin in terms of preantral follicle volumes in the present study, may be due to those authors using diameter measurement (the two-dimensional approach) when evaluating follicles, whereas we used volume calculation (the three-dimensional approach) to evaluate follicle size.

Vascularization and blood flow in the ovary are indispensable for adequate growth and development of ovarian follicles, ovulation, and corpus luteum formation (Behrman et al. 2001). In the present study, the blood vessel volume in the DM group was significantly lower compared with that in the control group. In our study, we think that the decrease in blood vessel volume in the ovarian tissue of the diabetes group is related to the decrease in the volume and number of developing follicles. It is thought that the decrease in ovarian stromal vascularity may lead to less delivery of gonadotropins to the granulosa cells of the developing follicles. During follicular atresia, the interruption of oxygen support through the blood vessels in the structure can initiate atresia. Images obtained from light microscopic and transmission electron microscopic examinations also support the above findings. The presence of capillaries with partially enlarged lumens in the theca follicle, which contains blood vessels of different diameters in the structure of the ovaries of the DM group, the fact that the capillaries are filled with amorphous material, and the intercellular space between the theca cells (disruption of the normal structure) shows that diabetes

adversely affects the blood vessels in the ovaries. It has been observed that there are similar structural defects in the lumens of the blood vessels in the ovarian medulla, which has loose connective tissue characteristics. The remarkable changes included the presence of amorphous substance in the reticular structure in the lumen of blood vessels due to the increase in blood viscosity, and the observation of many irregular protrusions on the endothelial surface facing the lumen. All these findings can be considered as causes of atresia and apoptosis-related factors in follicles.

Wu et al. (2017) reported that diabetic mice given a 20-week high-fat diet had low-density blood vessels in their ovaries, and that diabetes suppressed ovarian angiogenesis. Diabetes has been found to inhibit the expression of VEGF, a vital regulatory factor for angiogenesis. We attribute the decrease in blood vessel volume in diabetic group ovarian tissue in the present study to the decrease in the volume and number of developing follicles. A reduction in ovarian stromal vascularity may lead to less transmission of gonadotropins to the granulosa cells of the developing follicles.

Both clinical and experimental diabetes are known to impair endothelial-dependent vascular activity by inactivating NO (Cai et al. 2021). NO has a luteolytic effect, mediating the increase of prostaglandins in the corpus luteum (Fridén et al. 2000). Defects in the vessels that provide blood support in the corpus luteum prevent sufficient blood from reaching the luteal cells, which causes changes in progesterone secretion, resulting in insufficient luteal function in the corpus luteum (Hazzard et al. 2002). Corpus luteum volumes were calculated in the present study, and a significant decrease was observed in the DM group compared with the control, sham, and curcumin groups. A considerable increase was observed in the volume of the corpus luteum in the DC2 and DC3 groups compared with the DM group, while no difference was found between the DC1 group and the DM group. The corpus luteum volumes in the DC1 and DC3 groups exhibited a significant decrease compared with the control group corpus luteum. It was observed that there was no difference between the DC2 group and the control group in terms of corpus luteum volumes.

A decrease in the volume of the corpus luteum is known to lead to a reduction in progesterone concentrations (Gomez-Seco et al. 2017). A study in which experimental diabetes was induced with STZ (50 mg/kg) reported a decrease in the number and diameter of the corpus luteum in the diabetic group compared with the controls (Farhad et al. 2013). Apoptosis may occur in luteal cells due to hyperglycemia in the corpus luteum. In addition, the decrease in the volume of the corpus luteum may be due to reduced lipid reserves in luteal cells. It has also been suggested that curcumin can increase serum adiponectin and leptin levels in patients with metabolic syndrome (Panahi et al. 2016).

Improving the decreased lipid reserves of luteal cells by regulating plasma leptin levels with curcumin treatment may be the main mechanism involved in the preservation of corpus luteum volume. Further studies are now needed to investigate the effect of leptin levels on corpus luteum functions in diabetic individuals treated with curcumin.

The results of the present study suggest that curcumin may have protective effects on the ovary. In the present study, we found that curcumin positively promoted angiogenesis after long-term diabetes (21 days) when used concurrently with diabetes induction, although we did not expect a positive contribution to angiogenesis with curcumin administration 7 days after diabetes induction. We think that this bidirectional effect of curcumin on angiogenesis is regulated by the interaction of many factors, including VEGF, MMPs, TGF-1, and fibroblast growth factor (Wang and Chen 2019). The mechanism(s) underlying the opposite effect of curcumin on angiogenesis under different diabetic conditions now need to be investigated.

Examination of the vascular structure of the DC2 and DC3 groups under light microscopy revealed that the endothelium was normal in structure and very well bonded to the basement membrane due to the protective properties of curcumin. The presence of numerous pinocytic vesicles on the surface of the endothelial cells facing the basement membrane in these groups indicates that these cells are also functionally active.

The volume of ovarian connective tissue in the DM group increased significantly compared with the control and sham groups. In addition, no significant difference was found between the DM group and the curcumin group. The increase in the DM group ovarian connective tissue volume can be attributed to the fibrotic effect and inflammation regulated by TGF-1 and NF-kB. This may be one of the reasons for an adverse impact on ovarian functions. Because these factors increase in diabetic tissues in response to AGEs or high glucose levels (Erbas et al. 2014; Khedr 2017).

The increase in the volume of connective tissue in the ovary due to excessive proliferation of fibroblasts and the accumulation of extracellular matrix is one of the main causes of ovarian dysfunction (Zhou et al. 2017). In the present study, connective tissue volume decreased significantly after curcumin administration in the DC1, DC2, and DC3 groups compared with the DM group. These results suggest that curcumin normalizes female oocyte/follicle maturation in diabetic individuals by preventing fibrosis in the ovary. In addition, the absence of a significant difference in connective tissue volumes between these three groups (DC1, DC2, and DC3) and the control, sham, and curcumin groups suggest that curcumin administration normalizes the amount of connective tissue in the diabetic groups comparison with the control, sham, and curcumin groups. In addition, no difference was observed between the connective tissue volumes

of the control and sham groups and those of the curcumin group.

While there was no difference in ovarian cortex volumes in the DC1, DC2, and DC3 groups compared with the DM group, a significant decrease was observed in the DC1 and DC2 groups compared with the control group. This was directly proportional to the decrease in follicle numbers and connective tissue volume.

Functions such as follicular growth, oocyte maturation, and estrus behavior in the ovary are regulated by the action of gonadotropins (FSH and LH). The HPG axis has been shown to be adversely affected by diabetic conditions (Castellano et al. 2006, 2009). Hypothalamic–pituitary dysfunction in diabetic animals is characterized by low basal FSH and LH levels (Arrais and Dib 2006). Curcumin is known to exhibit phytoestrogenic effects (Bachmeier et al. 2010). It is therefore capable of regulating the endocrine function of reproduction by interacting with the endocrine system and affecting the HPG axis, and by supporting follicular development or the protection of follicles (Sirotkin and Harrath 2014; Yan et al. 2018). Curcumin has been reported to protect against pro-apoptotic, pronecrotic, antiproliferative, and anti-oogenic effects induced by suppression of FSH receptors in mouse ovary cells (Tiwari-Pandey and Ram Sairam 2009).

Examination of the effects of curcumin treatment applied at different times of diabetes on the HPG axis revealed that serum FSH levels increased significantly in the DC1 and DC3 groups compared with the DM group, but there was no difference between these two groups compared with the control group. On the basis of our findings, it may be concluded that curcumin brings FSH levels closer to normal when administered in parallel with the development of diabetes (DC3) or 7 days later (DC1). Serum FSH levels could not be normalized when curcumin was used after long-term diabetes (application 21 days after the onset of diabetes). It has been suggested that impairments in the reproductive function of diabetic female rats may be partially related to the secretion of gonadotropins or to a decrease in the affinity or number of gonadotropin receptors in ovarian target cells (Arrais and Dib 2006). The antioxidant effect of curcumin in the DC2 group may have been insufficient to prevent disorders in the affinity and/or numbers of gonadotropins; the secretion is reduced under long-term diabetic conditions. This may be due to the low dose of curcumin dose we used, or to the duration being insufficient. We think that the antioxidant effects of curcumin on serum FSH levels should now be investigated in studies focusing on dosage and duration.

Examination of serum LH levels revealed no difference between the DC1 and DC3 groups and the control, sham, curcumin, DM, or DC2 groups, while serum LH levels in the DC2 group were significantly lower than in the control, sham, and curcumin groups. We concluded that curcumin was insufficient to normalize serum LH levels under prolonged diabetic conditions (the DC2 group).

Previous studies have shown that oxidative stress may cause infertility by affecting numbers of ovarian follicles and oocytes (Miyamoto et al. 2010; Mehrabianfar et al. 2020). In the present study, CAT activity and SOD were measured to determine the underlying mechanism involved in decreased primordial/preantral follicle numbers, blood vessel volumes, and corpus luteum volumes in the diabetic groups. A significant increase in CAT activity was observed in the diabetic groups compared with the control group. In another study, and consistent with our own findings, CAT enzyme activity, which catalyzes the reduction of hydroperoxides and protects mammalian cells against oxidative damage by playing a role in neutralizing ROS, was significantly higher in diabetic rats compared with controls (Qujeq and Rezvani 2007). Increased CAT activity with membrane protein and lipid damage has been reported to be caused by an increase in free radicals. It may therefore be concluded that the antioxidant defense system increases CAT enzyme activity as a result of oxidative stress in diabetic groups.

All the findings obtained in the present study confirm that this sequence of events is interconnected. The increase in CAT enzyme activity in connection with decreased FSH values in the diabetic group in the present study shows that the increase in follicular ROS affects hormone levels, oocyte development, and follicle numbers. In that context, it may be concluded that a delicate balance exists between the synthesis and release of ovarian hormones or changes in the sensitivity of cells to hormones and antioxidant enzymes (Yan et al. 2022). The decrease in plasma SOD level in the diabetic groups in the present study may have occurred due to the increased oxidative stress in the ovary. A decrease in SOD levels may cause DNA damage in primordial/preantral and antral follicles, resulting in cell loss.

CAT activity and serum SOD levels were evaluated to investigate the effectiveness of curcumin, an antioxidant substance, against the decrease in follicle numbers caused by oxidative stress induced by diabetes and changes in ovarian structure. Accordingly, a significant decrease in CAT activity was observed in the DC2 and DC3 groups compared with the DM group, but no difference was found compared with the control group. Serum SOD levels increased significantly in the DM group compared with the DC1, DC2, and DC3 groups. The antioxidant effects of curcumin can occur through various mechanisms. One of the most important of these may be increasing the levels of intracellular antioxidants and their mRNA levels, which are adversely affected by diabetic conditions. Due to its antioxidant activity, curcumin may reduce oxidative-stress-induced toxicity, which adversely affects ovarian function, by normalizing intracellular antioxidant enzymes. In one study, high oxidative stress marker levels and decreased endogenous antioxidants

were observed in the ovaries of PCOS animals. The authors reported significant normalization of SOD, CAT, and GSH activities in the PCOS group with curcumin treatment (Reddy et al. 2016).

Conclusion

The findings of the present study indicate that diabetes causes a decrease in the number of follicles in the ovary, follicle and corpus luteum volumes, blood vessel and ovarian cortex volumes, body weight, GSI, and serum SOD and FSH levels. In addition, diabetes causes an increase in CAT activity and connective tissue volume. Curcumin, which possesses powerful antioxidant properties, was used to eliminate this adverse manifestation caused by diabetes. The protective effect of this substance in different stages of diabetes was extensively investigated using stereological, biochemical, and histopathological analyses. It may therefore be concluded that curcumin exerts its protective effects on diabetic ovaries using the following mechanisms;

- Regulation of the HPG axis,
- Preservation of the ovarian cycle and follicle numbers,
- Maintenance of the normal structure of the blood vessel, and
- Reduction of fibrosis in the ovary and lowering hyperglycemia

The findings suggest that curcumin may be a desirable and effective substance for restoring ovarian follicle damage in individuals exposed to hyperglycemia. However, comprehensive molecular studies are now needed on this subject. In addition, it should not be forgotten that, in addition to its antioxidant properties, curcumin might also have a pro-oxidant effect under some conditions.

Author contributions K.K.T.: conceived and designed the study, performed the experiment, and analyzed the data under the supervision of S.K. S.K. also managed the funding acquisition and administered all stages of the project. All authors contributed towards the interpretation of findings from this study, played a role in drafting the article or revising it critically for its intellectual content, and gave their final approval for this version of the paper to be published.

Declarations

Conflict of interest The author declares that there is no conflict of interest.

References

Abu-Taweel GM, Rudayni HA (2022) Curcumin ameliorated the mercuric chloride induced depression and anxiety in female mice offspring. Environ Res 204(Pt B):112031. https://doi.org/10.1016/j.envres.2021.112031

Adab Z, Eghtesadi S, Vafa MR, Heydari I, Shojaii A, Haqqani H, Arablou T, Eghtesadi M (2019) Effect of turmeric on glycemic status, lipid profile, hs-CRP, and total antioxidant capacity in hyperlipidemic type 2 diabetes mellitus patients. Phytother Res 33(4):1173–1181. https://doi.org/10.1002/ptr.6312

Ahn J, Lee H, Kim S, Ha T (2010) Curcumin-induced suppression of adipogenic differentiation is accompanied by activation of Wnt/beta-catenin signaling. Am J Physiol Cell Physiol 298(6):C1510-1516. https://doi.org/10.1152/ajpcell.00369.2009

Aktas C, Kanter M, Kocak Z (2012) Antiapoptotic and proliferative activity of curcumin on ovarian follicles in mice exposed to whole body ionizing radiation. Toxicol Ind Health 28(9):852–863. https://doi.org/10.1177/0748233711425080

Andrade Cetto A, Wiedenfeld H, Revilla MC, Sergio IA (2000) Hypoglycemic effect of *Equisetum myriochaetum* aerial parts on streptozotocin diabetic rats. J Ethnopharmacol 72(1–2):129–133

Arrais RF, Dib SA (2006) The hypothalamus–pituitary–ovary axis and type 1 diabetes mellitus: a mini review. Hum Reprod 21(2):327–337. https://doi.org/10.1093/humrep/dei353

Asadi S, Gholami MS, Siassi F, Qorbani M, Sotoudeh G (2020) Beneficial effects of nano-curcumin supplement on depression and anxiety in diabetic patients with peripheral neuropathy: a randomized, double-blind, placebo-controlled clinical trial. Phytother Res 34(4):896–903. https://doi.org/10.1002/ptr.6571

Awadin WF, Merghani BH, Elseady YY, Abu-Heakal SAN (2015) Protective role of wheat germ oil against hyperglycemia and hyperlipidemia in streptozotocin induced diabetic rats. Asian J Anim Vet Adv 10(12):852–864. https://doi.org/10.3923/ajava.2015.852.864

Bachmeier BE, Mirisola V, Romeo F, Generoso L, Esposito A, Dell'eva R, Blengio F, Killian PH, Albini A, Pfeffer U (2010) Reference profile correlation reveals estrogen-like trancriptional activity of curcumin. Cell Physiol Biochem 26(3):471–482. https://doi.org/10.1159/000320570

Ballester J, Muñoz MC, Domínguez J, Palomo MJ, Rivera M, Rigau T, Guinovart JJ, Rodríguez-Gil JE (2007) Tungstate administration improves the sexual and reproductive function in female rats with streptozotocin-induced diabetes. Hum Reprod 22(8):2128–2135. https://doi.org/10.1093/humrep/dem168

Behrman HR, Kodaman PH, Preston SL, Gao S (2001) Oxidative stress and the ovary. J Soc Gynecol Investig 8(1):S40-42

Behroozi-Lak T, Ebrahimpour M, Zarei L, Pourjabali M, Farhad N, Mohaddesi H (2018) Systemic administration of curcumin nanoparticles protects ischemia–reperfusion injury in ovaries: an animal model study. Rev Assoc Med Bras 64(1):22–31. https://doi.org/10.1590/1806-9282.64.01.22

Boyce RW, Dorph-Petersen K-A, Lyck L, Gundersen HJG (2010) Design-based stereology. Toxicol Pathol 38(7):1011–1025. https://doi.org/10.1177/0192623310385140

Cai Z, Yuan S, Zhong Y, Deng L, Li J, Tan X, Feng J (2021) Amelioration of endothelial dysfunction in diabetes: role of Takeda G protein-coupled receptor 5. Front Pharmacol 12:637051. https://doi.org/10.3389/fphar.2021.637051

Castellano JM, Navarro VM, Fernandez-Fernandez R, Roa J, Vigo E, Pineda R, Dieguez C, Aguilar E, Pinilla L, Tena-Sempere M (2006) Expression of hypothalamic KiSS-1 system and rescue of defective gonadotropic responses by kisspeptin in streptozotocin-induced diabetic male rats. Diabetes 55(9):2602–2610. https://doi.org/10.2337/db05-1584

Castellano JM, Navarro VM, Roa J, Pineda R, Sanchez-Garrido MA, Garcia-Galiano D, Vigo E, Dieguez C, Aguilar E, Pinilla L, Tena-Sempere M (2009) Alterations in hypothalamic KiSS-1 system in experimental diabetes: early changes and functional consequences. Endocrinology 150(2):784–794. https://doi.org/10.1210/en.2008-0849

Chang AS, Dale AN, Moley KH (2005) Maternal diabetes adversely affects preovulatory oocyte maturation, development, and granulosa cell apoptosis. Endocrinology 146(5):2445–2453. https://doi.org/10.1210/en.2004-1472

Codner E, Merino PM, Tena-Sempere M (2012) Female reproduction and type 1 diabetes: from mechanisms to clinical findings. Hum Reprod Update 18(5):568–585. https://doi.org/10.1093/humupd/dms024

Depmann M, Broer SL, van der Schouw YT, Tehrani FR, Eijkemans MJ, Mol BW, Broekmans FJ (2016) Can we predict age at natural menopause using ovarian reserve tests or mother's age at menopause? A systematic literature review. Menopause 23(2):224–232. https://doi.org/10.1097/GME.0000000000000509

El-Demerdash FM, Yousef MI, Radwan FME (2009) Ameliorating effect of curcumin on sodium arsenite-induced oxidative damage and lipid peroxidation in different rat organs. Food Chem Toxicol 47(1):249–254. https://doi.org/10.1016/j.fct.2008.11.013

Erbas O, Pala HG, Pala EE, Oltulu F, Aktug H, Yavasoglu A, Taskiran D (2014) Ovarian failure in diabetic rat model: nuclear factor-kappaB, oxidative stress, and pentraxin-3. Taiwan J Obstet Gynecol 53(4):498–503. https://doi.org/10.1016/j.tjog.2013.11.008

Farhad K, Shahla Z, Hossein K, Sara A, Mohammad F, Saeid M (2013) Stereological and histopathological study of ovarian tissue after hydro-alcoholic extract of *Artemisia* plants compared with metformin in diabetic rats. Adv Environ Biol 7(4):749–754

Ferguson JJA, Abbott KA, Garg ML (2021) Anti-inflammatory effects of oral supplementation with curcumin: a systematic review and meta-analysis of randomized controlled trials. Nutr Rev 79(9):1043–1066. https://doi.org/10.1093/nutrit/nuaa114

Fridén BE, Runesson E, Hahlin M, Brännström M (2000) Evidence for nitric oxide acting as a luteolytic factor in the human corpus luteum. MHR Basic Sci Reprod Med 6(5):397–403. https://doi.org/10.1093/molehr/6.5.397

Garris DR (1984) Effects of progressive hyperglycemia on ovarian structure and function in the spontaneously diabetic Chinese hamster. Anat Rec 210(3):485–489. https://doi.org/10.1002/ar.1092100309

Garris DR, Garris BL (2004) Cytolipotoxicity-induced involution of the female reproductive tract following expression of obese (ob/ob) and diabetes (db/db) genotype mutations: progressive, hyperlipidemic transformation into adipocytic tissues. Reprod Toxicol 18(1):81–91. https://doi.org/10.1016/j.reprotox.2003.10.001

Gomez-Seco C, Alegre B, Martinez-Pastor F, Prieto JG, Gonzalez-Montana JR, Alonso ME, Dominguez JC (2017) Evolution of the corpus luteum volume determined ultrasonographically and its relation to the plasma progesterone concentration after artificial insemination in pregnant and non-pregnant dairy cows. Vet Res Commun 41(3):183–188. https://doi.org/10.1007/s11259-017-9685-x

Gundersen HJ (1986) Stereology of arbitrary particles. A review of unbiased number and size estimators and the presentation of some new ones, in memory of William R Thompson. J Microsc 143(1):3–45

Gundersen HJ, Jensen EB (1987) The efficiency of systematic sampling in stereology and its prediction. J Microsc 147(Pt 3):229–263

Hazzard TM, Xu F, Stouffer RL (2002) Injection of soluble vascular endothelial growth factor receptor 1 into the preovulatory follicle disrupts ovulation and subsequent luteal function in rhesus monkeys. Biol Reprod 67(4):1305–1312. https://doi.org/10.1095/biolreprod67.4.1305

Herman WH (2007) Diabetes epidemiology: guiding clinical and public health practice: the Kelly West Award Lecture, 2006. Diabetes Care 30(7):1912–1919. https://doi.org/10.2337/dc07-9924

Kamal DAM, Salamt N, Yusuf ANM, Kashim M, Mokhtar MH (2021) Potential health benefits of curcumin on female reproductive disorders: a review. Nutrients. https://doi.org/10.3390/nu13093126

Kandemir FM, Ozkaraca M, Küçükler S, Caglayan C, Hanedan B (2017) Preventive effects of hesperidin on diabetic nephropathy induced by streptozotocin via modulating TGF-β1 and oxidative DNA damage. Toxin Rev 37(4):287–293. https://doi.org/10.1080/15569543.2017.1364268

Kezele PR, Nilsson EE, Skinner MK (2002) Insulin but not insulin-like growth factor-1 promotes the primordial to primary follicle transition. Mol Cell Endocrinol 192(1–2):37–43

Khaksar Z, Jelodar G, Hematian H, Poorahmadi M (2013) Alterations of the ovarian histomorphometry at pre-puberty in rat offspring from diabetic mothers. Reprod Med Biol 12(4):173–178. https://doi.org/10.1007/s12522-013-0151-3

Khedr NF (2017) Fish oil and wheat-germ oil supplementation restores ovarian function in streptozotocin-diabetic rats. Reprod Fertil Dev 29(9):1689. https://doi.org/10.1071/rd16135

Kim NN, Stankovic M, Cushman TT, Goldstein I, Munarriz R, Traish AM (2006) Streptozotocin-induced diabetes in the rat is associated with changes in vaginal hemodynamics, morphology and biochemical markers. BMC Physiol 6(1):4. https://doi.org/10.1186/1472-6793-6-4

Kovacevic M, Malis S, Pavlovic D, Kovacevic M, Savic Radojevic A, Djukanovic L (2022) Plasma activity of the antioxidant enzymes in predicting diabetic nephropathy progression. Int Urol Nephrol 54(6):1365–1372. https://doi.org/10.1007/s11255-021-03031-1

Lin YG, Kunnumakkara AB, Nair A, Merritt WM, Han LY, Armaiz-Pena GN, Kamat AA, Spannuth WA, Gershenson DM, Lutgendorf SK, Aggarwal BB, Sood AK (2007) Curcumin inhibits tumor growth and angiogenesis in ovarian carcinoma by targeting the nuclear factor-kappaB pathway. Clin Cancer Res 13(11):3423–3430. https://doi.org/10.1158/1078-0432.CCR-06-3072

Liu S, Liu J, He L, Liu L, Cheng B, Zhou F, Cao D, He Y (2022) A comprehensive review on the benefits and problems of curcumin with respect to human health. Molecules. https://doi.org/10.3390/molecules27144400

Marton LT, Pescinini ESLM, Camargo MEC, Barbalho SM, Haber J, Sinatora RV, Detregiachi CRP, Girio RJS, Buchaim DV, Dos Santos C, Bueno P (2021) The effects of curcumin on diabetes mellitus: a systematic review. Front Endocrinol 12:669448. https://doi.org/10.3389/fendo.2021.669448

Meghana K, Sanjeev G, Ramesh B (2007) Curcumin prevents streptozotocin-induced islet damage by scavenging free radicals: a prophylactic and protective role. Eur J Pharmacol 577(1–3):183–191. https://doi.org/10.1016/j.ejphar.2007.09.002

Mehrabianfar P, Dehghani F, Karbalaei N, Mesbah F (2020) The effects of metformin on stereological and ultrastructural features of the ovary in streptozotocin-induced diabetes adult rats: an experimental study. Int J Reprod Biomed 18(8):651–666. https://doi.org/10.18502/ijrm.v13i8.7506

Memarzia A, Khazdair MR, Behrouz S, Gholamnezhad Z, Jafarnezhad M, Saadat S, Boskabady MH (2021) Experimental and clinical reports on anti-inflammatory, antioxidant, and immunomodulatory effects of *Curcuma longa* and curcumin, an updated and comprehensive review. BioFactors 47(3):311–350. https://doi.org/10.1002/biof.1716

Miyamoto K, Sato EF, Kasahara E, Jikumaru M, Hiramoto K, Tabata H, Katsuragi M, Odo S, Utsumi K, Inoue M (2010) Effect of oxidative stress during repeated ovulation on the structure and functions of the ovary, oocytes, and their mitochondria. Free Radic

Biol Med 49(4):674–681. https://doi.org/10.1016/j.freeradbiomed.2010.05.025

Myers M, Britt KL, Wreford NGM, Ebling FJP, Kerr JB (2004) Methods for quantifying follicular numbers within the mouse ovary. Reproduction 127(5):569–580. https://doi.org/10.1530/rep.1.00095

Nabavi S, Thiagarajan R, Rastrelli L, Daglia M, Sobarzo-Sanchez E, Alinezhad H, Nabavi S (2015) Curcumin: a natural product for diabetes and its complications. Curr Top Med Chem 15(23):2445–2455. https://doi.org/10.2174/1568026615666150619142519

Oluwatoyin AO, Olugbenga OM, Peter FA, David O (2013) Gonadosomatic index of female Wister rats treated with graded concentration of Aloe Vera gel. J Med Plants Res 7:339–342

Panahi Y, Hosseini MS, Khalili N, Naimi E, Soflaei SS, Majeed M, Sahebkar A (2016) Effects of supplementation with curcumin on serum adipokine concentrations: a randomized controlled trial. Nutrition 32(10):1116–1122. https://doi.org/10.1016/j.nut.2016.03.018

Perez-Torres I, Ruiz-Ramirez A, Banos G, El-Hafidi M (2013) *Hibiscus sabdariffa* Linnaeus (Malvaceae), curcumin and resveratrol as alternative medicinal agents against metabolic syndrome. Cardiovasc Hematol Agents Med Chem 11(1):25–37

Pralong FP (2010) Insulin and NPY pathways and the control of GnRH function and puberty onset. Mol Cell Endocrinol 324(1–2):82–86. https://doi.org/10.1016/j.mce.2010.01.037

Prasad SK, Kulshresht A, Qureshi NT (2009) Antidiabetic activity of some herbal plants in streptozotocin induced diabetic albino rats. Pak J Nutr 8(5):551–557. https://doi.org/10.3923/pjn.2009.551.557

Qujeq D, Rezvani T (2007) Catalase (antioxidant enzyme) activity in streptozotocin-induced diabetic rats. Int J Diabetes Metab 15:22–24

Reddy PS, Begum N, Mutha S, Bakshi V (2016) Beneficial effect of curcumin in letrozole induced polycystic ovary syndrome. Asian Pac J Reprod 5(2):116–122. https://doi.org/10.1016/j.apjr.2016.01.006

Sak ME, Soydinc HE, Sak S, Evsen MS, Alabalik U, Akdemir F, Gul T (2013) The protective effect of curcumin on ischemia–reperfusion injury in rat ovary. Int J Surg 11(9):967–970. https://doi.org/10.1016/j.ijsu.2013.06.007

Shafabakhsh R, Asemi Z, Reiner Z, Soleimani A, Aghadavod E, Bahmani F (2020) The effects of nano-curcumin on metabolic status in patients with diabetes on hemodialysis, a randomized, double blind, placebo-controlled trial. Iran J Kidney Dis 14(4):290–299

Sharma S, Kulkarni SK, Chopra K (2006) Curcumin, the active principle of turmeric (*Curcuma longa*), ameliorates diabetic nephropathy in rats. Clin Exp Pharmacol Physiol 33(10):940–945. https://doi.org/10.1111/j.1440-1681.2006.04468.x

Shima H, Naeem E, Hassan M, Hossein N (2011) Aloe vera gel protects ovarian structure in diabetic rat. Am-Eurasian J Toxicol Sci 3:197–203

Sirotkin AV, Harrath AH (2014) Phytoestrogens and their effects. Eur J Pharmacol 741:230–236. https://doi.org/10.1016/j.ejphar.2014.07.057

Sirotkin AV, Kadasi A, Stochmalova A, Balazi A, Földesiová M, Makovicky P, Chrenek P, Harrath AH (2017) Effect of turmeric on the viability, ovarian folliculogenesis, fecundity, ovarian hormones and response to luteinizing hormone of rabbits. Animal 12(06):1242–1249. https://doi.org/10.1017/s175173111700235x

Soleimani V, Sahebkar A, Hosseinzadeh H (2018) Turmeric (*Curcuma longa*) and its major constituent (curcumin) as nontoxic and safe substances: review. Phytother Res 32(6):985–995. https://doi.org/10.1002/ptr.6054

Tiwari-Pandey R, Ram Sairam M (2009) Modulation of ovarian structure and abdominal obesity in curcumin- and flutamide-treated aging FSH-R haploinsufficient mice. Reprod Sci 16(6):539–550. https://doi.org/10.1177/1933719109332822

Valdes CT, Elkind-Hirsch KE, Rogers DG, Adelman JP (1991) The hypothalamic–pituitary axis of streptozotocin-induced diabetic female rats is not normalized by estradiol replacement*. Endocrinology 128(1):433–440. https://doi.org/10.1210/endo-128-1-433

Volpe CMO, Villar-Delfino PH, dos Anjos PMF, Nogueira-Machado JA (2018) Cellular death, reactive oxygen species (ROS) and diabetic complications. Cell Death Dis. https://doi.org/10.1038/s41419-017-0135-z

Walker DM, Kermath BA, Woller MJ, Gore AC (2013) Disruption of reproductive aging in female and male rats by gestational exposure to estrogenic endocrine disruptors. Endocrinology 154(6):2129–2143. https://doi.org/10.1210/en.2012-2123

Wang TY, Chen JX (2019) Effects of curcumin on vessel formation insight into the pro- and antiangiogenesis of curcumin. Evid Based Complement Alternat Med 2019:1390795. https://doi.org/10.1155/2019/1390795

Wang M, Su P (2018) The role of the Fas/FasL signaling pathway in environmental toxicant-induced testicular cell apoptosis: an update. Syst Biol Reprod Med 64(2):93–102. https://doi.org/10.1080/19396368.2017.1422046

Wu Y, Li Y, Liao X, Wang Z, Li R, Zou S, Jiang T, Zheng B, Duan P, Xiao J (2017) Diabetes induces abnormal ovarian function via triggering apoptosis of granulosa cells and suppressing ovarian angiogenesis. Int J Biol Sci 13(10):1297–1308. https://doi.org/10.7150/ijbs.21172

Xie T, Chen X, Chen W, Huang S, Peng X, Tian L, Wu X, Huang Y (2021) Curcumin is a potential adjuvant to alleviates diabetic retinal injury via reducing oxidative stress and maintaining Nrf2 pathway homeostasis. Front Pharmacol 12:796565. https://doi.org/10.3389/fphar.2021.796565

Yan Z, Dai Y, Fu H, Zheng Y, Bao D, Yin Y, Chen Q, Nie X, Hao Q, Hou D, Cui Y (2018) Curcumin exerts a protective effect against premature ovarian failure in mice. J Mol Endocrinol 60(3):261–271. https://doi.org/10.1530/jme-17-0214

Yan F, Zhao Q, Li Y, Zheng Z, Kong X, Shu C, Liu Y, Shi Y (2022) The role of oxidative stress in ovarian aging: a review. J Ovarian Res 15(1):100. https://doi.org/10.1186/s13048-022-01032-x

Yavas Y, Selub MR (2009) Ovarian follicular volume and follicular surface area are better indicators of follicular growth and maturation, respectively, than is follicular diameter. Fertil Steril 91(4):1299–1302. https://doi.org/10.1016/j.fertnstert.2008.01.050

Yuan X, Ni H, Chen X, Feng X, Wu Q, Chen J (2018) Identification of therapeutic effect of glucagon-like peptide 1 in the treatment of STZ-induced diabetes mellitus in rats by restoring the balance of intestinal flora. J Cell Biochem 119(12):10067–10074. https://doi.org/10.1002/jcb.27343

Zhang DW, Fu M, Gao SH, Liu JL (2013) Curcumin and diabetes: a systematic review. Evid Based Complement Alternat Med 2013:636053. https://doi.org/10.1155/2013/636053

Zhao J, Sun XB, Ye F, Tian WX (2011) Suppression of fatty acid synthase, differentiation and lipid accumulation in adipocytes by curcumin. Mol Cell Biochem 351(1–2):19–28. https://doi.org/10.1007/s11010-010-0707-z

Zhou F, Shi L-B, Zhang S-Y (2017) Ovarian fibrosis. Chin Med J 130(3):365–371. https://doi.org/10.4103/0366-6999.198931